



## RESEARCH ARTICLE

# A drained nutrient-poor peatland forest in boreal Sweden constitutes a net carbon sink after integrating terrestrial and aquatic fluxes

Cheuk Hei Marcus Tong<sup>1</sup>  | Koffi Dodji Noumonvi<sup>1</sup> | Joshua Ratcliffe<sup>1,2</sup> |  
Hjalmar Laudon<sup>1</sup> | Järvi Järveoja<sup>1</sup>  | Andreas Drott<sup>3</sup> | Mats B. Nilsson<sup>1</sup>  |  
Matthias Peichl<sup>1</sup> 

<sup>1</sup>Department of Forest Ecology and Management, Swedish University of Agricultural Sciences, Umeå, Sweden

<sup>2</sup>Unit for Field-Based Forest Research, Swedish University of Agricultural Sciences, Vindeln, Sweden

<sup>3</sup>The Swedish Forest Agency, Umeå, Sweden

## Correspondence

Cheuk Hei Marcus Tong, Department of Forest Ecology and Management, Swedish University of Agricultural Sciences, 901 83 Umeå, Sweden.

Email: [cheuk.hei.tong@slu.se](mailto:cheuk.hei.tong@slu.se)

## Funding information

Stiftelsen Oscar och Lili Lamms Minne, Grant/Award Number: 2017.4.1-68; Knut och Alice Wallenbergs Stiftelse, Grant/Award Number: 2018.0259; Kempestiftelserna, Grant/Award Number: JCK-1712; Svenska Forskningsrådet Formas, Grant/Award Number: 2016-01289, 2017-00635 and 2020-01446; Swedish University of Agricultural Sciences

## Abstract

Northern peatlands provide a globally important carbon (C) store. Since the beginning of the 20th century, however, large areas of natural peatlands have been drained for biomass production across Fennoscandia. Today, drained peatland forests constitute a common feature of the managed boreal landscape, yet their ecosystem C balance and associated climate impact are not well understood, particularly within the nutrient-poor boreal region. In this study, we estimated the net ecosystem carbon balance (NECB) from a nutrient-poor drained peatland forest and an adjacent natural mire in northern Sweden by integrating terrestrial carbon dioxide (CO<sub>2</sub>) and methane (CH<sub>4</sub>) fluxes with aquatic losses of dissolved organic C (DOC) and inorganic C based on eddy covariance and stream discharge measurements, respectively, over two hydrological years. Since the forest included a dense spruce-birch area and a sparse pine area, we were able to further evaluate the effect of contrasting forest structure on the NECB and component fluxes. We found that the drained peatland forest was a net C sink with a 2-year mean NECB of  $-115 \pm 5 \text{ g C m}^{-2} \text{ year}^{-1}$  while the adjacent mire was close to C neutral with  $14.6 \pm 1.7 \text{ g C m}^{-2} \text{ year}^{-1}$ . The NECB of the drained peatland forest was dominated by the net CO<sub>2</sub> exchange (net ecosystem exchange [NEE]), whereas NEE and DOC export fluxes contributed equally to the mire NECB. We further found that the C sink strength in the sparse pine forest area ( $-153 \pm 8 \text{ g C m}^{-2} \text{ year}^{-1}$ ) was about 1.5 times as high as in the dense spruce-birch forest area ( $-95 \pm 8 \text{ g C m}^{-2} \text{ year}^{-1}$ ) due to enhanced C uptake by ground vegetation and lower DOC export. Our study suggests that historically drained peatland forests in nutrient-poor boreal regions may provide a significant net ecosystem C sink and associated climate benefits.

## KEYWORDS

boreal peatland, carbon balance, CH<sub>4</sub>, CO<sub>2</sub>, DIC, DOC, forestry drainage

This is an open access article under the terms of the [Creative Commons Attribution](https://creativecommons.org/licenses/by/4.0/) License, which permits use, distribution and reproduction in any medium, provided the original work is properly cited.

© 2024 The Authors. *Global Change Biology* published by John Wiley & Sons Ltd.

## 1 | INTRODUCTION

Peatlands are the most widespread type of wetlands globally (Joosten & Clarke, 2002) and provide an important long-term sink for carbon (C) due to a persistent positive imbalance between the C input through net primary production and loss via organic matter decomposition (Clymo, 1984). However, anthropogenic activities have altered the peatland C cycle and associated climate impact (Turetsky et al., 2002). Specifically, up to 35% of 20Mha of peatland in Fennoscandia have been drained since the beginning of the 20th century with the goal to increase timber production (Eliasson, 2008; Paavilainen & Päivänen, 1995). These drainage activities are well documented to enhance peat decomposition and associated soil C losses (Laine et al., 1995), due to which drained peatland forests are considered by default as C sources in national emission reporting (Hiraishi et al., 2014). The few studies exploring the ecosystem-scale C balance (i.e. including soil and tree C fluxes) of northern peatland forests, however, suggest that while some of these areas act as C sources (Laine et al., 2019; Lohila et al., 2007), others constitute significant C sinks (Lohila et al., 2011; Meyer et al., 2013; Ojanen et al., 2013). Thus, there is a need to improve our knowledge of the ecosystem C balance and associated climate impact of drained boreal peatland forests.

Soil fertility, hydrology and climate appear as key factors determining the variations in the C balance of boreal peatland forests. Specifically, peat mineralization and subsequent carbon dioxide (CO<sub>2</sub>) emission rates are commonly higher in nutrient-rich, well-drained soils and/or warmer climate regions, compared to nutrient-poor soils, higher water levels and/or colder regions (Ojanen et al., 2013; Silvola, 1986). At present, however, data on the annual ecosystem-scale C balance of northern peatland forests exist primarily from a fertile hemi-boreal site (Meyer et al., 2013) as well as from a fertile (Lohila et al., 2007) and infertile site (Lohila et al., 2011; Minkkinen et al., 2018) in the southern boreal region. In comparison, data for the relatively larger middle and northern boreal regions (Ahti et al., 1968) are limited to only one but extensive study of a north–south transect across Finland (Ojanen et al., 2013). While that study combined chamber measurements of soil fluxes during the snow-free season with tree production estimates, year-round and direct measurements of the ecosystem-scale C balance using the eddy covariance (EC) technique (Baldocchi, 2003) are lacking for peatland forests in the more nutrient-poor middle and northern boreal regions. Given large gradients in soil fertility (Callesen et al., 2007), hydrology (Laudon & Hasselquist, 2023) and climatic conditions across Fennoscandia, a comprehensive database is critical for a better understanding of how these key factors regulate the C balance of drained peatland forests across the boreal biome.

Apart from its effects on CO<sub>2</sub> fluxes, drainage also alters methane (CH<sub>4</sub>) production and oxidation dynamics. Specifically, drained peatland forests commonly have lower CH<sub>4</sub> emissions compared to pristine mire sites and may even act as a sink of CH<sub>4</sub> (Korkiakoski et al., 2017; Lohila et al., 2011). Considering its powerful warming

potential relative to CO<sub>2</sub> (i.e. 81 and 28 times higher during a 20- and 100-year time frame, respectively; IPCC, 2022), changes in CH<sub>4</sub> fluxes may strongly modify the net climate impact of peatland forestry. Yet, while previous CH<sub>4</sub> flux estimates in drained boreal peatland forests rely on chamber measurements of soil fluxes (Korkiakoski et al., 2017; Meyer et al., 2013; Ojanen et al., 2013), EC-based estimates of the whole ecosystem CH<sub>4</sub> exchange, capturing also potentially significant emissions via trees (Ranniku et al., 2023; Vainio et al., 2022) and from ditches (Peacock et al., 2021), are not available to date.

In addition to the terrestrial ecosystem–atmosphere exchange of C, the aquatic C export via discharge may represent another important but often overlooked component of the boreal peatland C cycle (Cole et al., 2007; Nilsson et al., 2008). Aquatic C fluxes in the form of dissolved organic C (DOC) and dissolved inorganic C (DIC; including dissolved CO<sub>2</sub> and CH<sub>4</sub>) are strongly coupled with vegetation structure and hydrological regime (Moore, 2003; Neubauer & Megonigal, 2021) and thus subject to change following drainage (Evans et al., 2016; Nieminen et al., 2021). However, while the aquatic C loss has been integrated with terrestrial fluxes to estimate the net ecosystem carbon balance (NECB; Chapin et al., 2006) for natural mires (Koehler et al., 2011; Nilsson et al., 2008; Roulet et al., 2007), such holistic assessment of the NECB has not been conducted for boreal drained peatland forests.

Variations in the C balance of drained peatland forests may also result from differences in forest structure. Specifically, tree density has been suggested as control of CO<sub>2</sub> (Alm et al., 2007; Badorek et al., 2011; Minkkinen et al., 2018), CH<sub>4</sub> (Minkkinen et al., 2007; Ojanen et al., 2010) and aquatic C flux dynamics (Finstad et al., 2016; Nieminen et al., 2021) in drained peatland ecosystems. In addition, feedbacks between tree transpiration rates and water table level (WTL) response may continuously improve the conditions for tree growth (Sikström & Hökkä, 2016) and modify aquatic C export dynamics (Laine et al., 1996; Pastor et al., 2003). Higher stand volume may also enhance the rate of root exudation and soil litter production, resulting in greater labile DOC pools and altered soil biogeochemistry (Palviainen et al., 2022). However, while previous studies noted tree density effects on individual C cycle components, the role of forest structure in regulating the integrated NECB of drained peatland forests remains unclear.

In this study, we combined data on the net ecosystem exchanges of CO<sub>2</sub> and CH<sub>4</sub> with aquatic C export estimates with the aim to assess the NECB of a drained forest peatland and an adjacent natural mire in the nutrient-poor boreal region of Northern Sweden. The specific objectives were to (1) quantify the annual NECB and the relative contributions of its individual component fluxes for a drained peatland forest and an adjacent natural mire, (2) compare the responses of the NECB component fluxes to key environmental variables in drained and natural peatlands and (3) evaluate the effect of forest structure (i.e. primarily tree density and species composition) on the NECB and its component fluxes in a drained peatland forest.

## 2 | MATERIALS AND METHODS

### 2.1 | Site description

This study was conducted at the Hälsingfors drained peatland forest (HDPF) (64°09' N, 19°33' E) and a nearby natural mire which are part of the Kulbäcksliden Research Infrastructure (Noumonvi et al., 2023), located in the municipality of Vindeln, county of Västerbotten, Northern Sweden (Figure 1). The study site is situated in the middle boreal region (Ahti et al., 1968), experiencing a 30-year mean (1990–2020) annual precipitation of 645 mm and a mean annual temperature of +3.0°C (based on climatic data from the nearby Kulbäcksliden reference station; 64°11'05" N 19°34'43" E, 275 m a.s.l.). The mean June and July temperatures are +12.6°C and +15.4°C, respectively. The length of the growing season, defined as the period in which daily temperature exceeds +5°C for three consecutive days with reference to the Swedish Meteorological and Hydrological Institute (SMHI), was 146 (26th May to 19th October), 132 (25th May to 4th October) and 156 days (14th May to 17 October) during the three measurement years 2020–2022.

The HDPF was originally an oligo-minerotrophic mire. Based on the analysis of 147 tree-ring samples, a substantial establishment of trees took place about 130 years ago, which likely corresponds to the time shortly after the drainage ditch network was established. No management or logging has occurred since drainage and natural tree seedling establishment, yet currently most ditches still maintain substantial drainage capacity. The northern part has a slightly higher altitude (~5 m), resulting in an active flow of water along the ditches from north to south. The site includes two distinct areas, located broadly east and west of the flux tower, which differ in tree density, species composition and volume. Specifically, the eastern area is characterized by a sparsely treed Scots pine (*Pinus sylvestris* L.) forest where *Sphagnum fuscum* dominates the forest floor. The western area resembles a relatively dense forest composed primarily of downy birch (*Betula pubescens* L.; 56% based on stem density) and Norway spruce (*Picea abies* L.; 37% based on stem density) species, where dwarf shrubs *Vaccinium myrtillus* L. and *V. vitis-idaea* as well as the forest mosses *Pleurozium schreberi* and *Dicranum* sp. dominate the forest floor vegetation (Table 1). The sparse and dense forest areas are classified as dwarf shrubs and bilberry-horsetail types, respectively, according to Hånell (1991). A tree

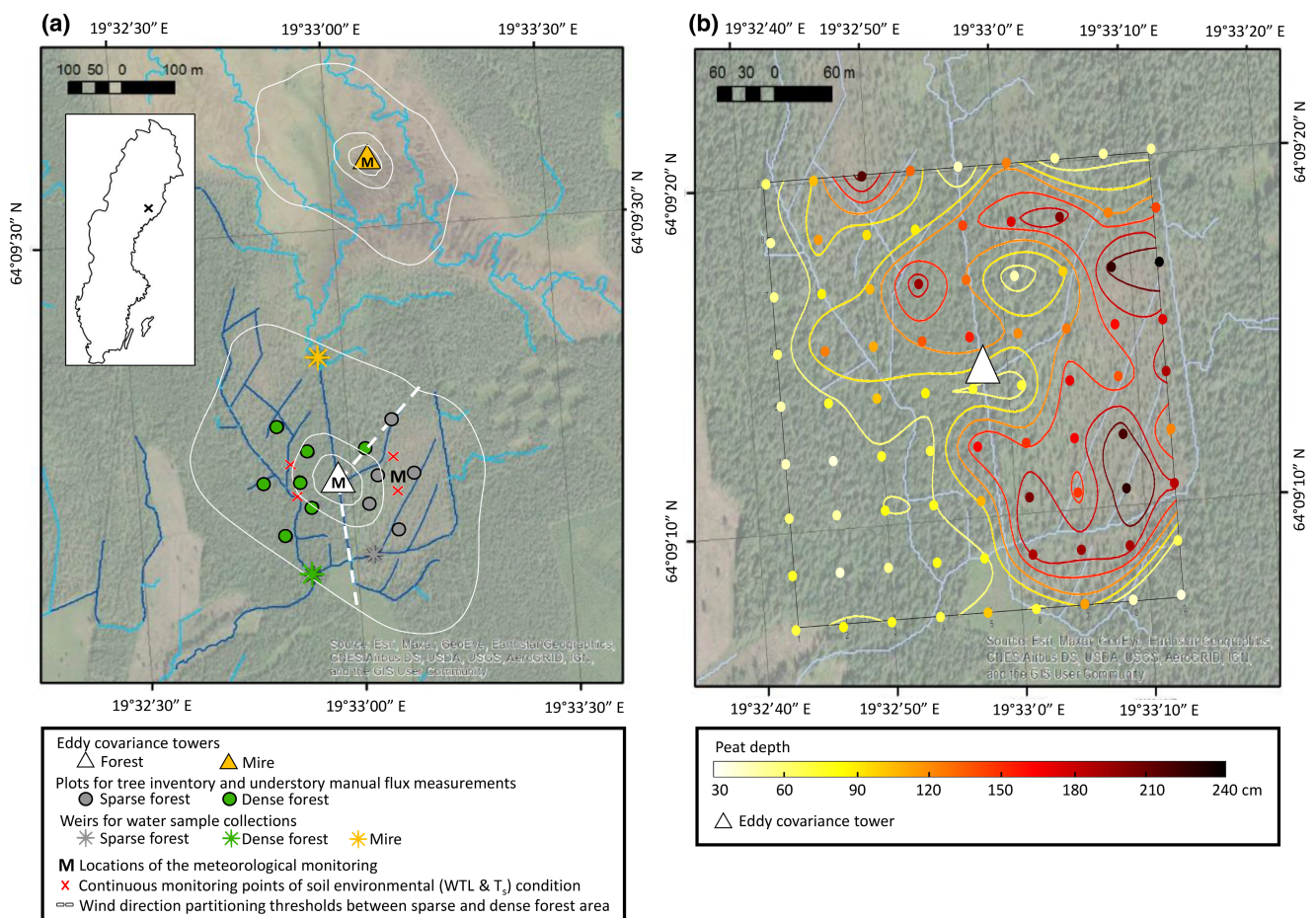


**FIGURE 1** (a) Geographical location and experimental setup at the Hälsingfors drained peatland forest and mire sites, and (b) peat depth distribution at the drained peatland forest area. In (a), the white contours around each tower denote the 50%, 70% and 90% footprint contours of the eddy covariance system using Flux Footprint Prediction (FFP) (Kljun et al., 2015). The light and dark blue lines denote the natural stream and man-made ditches, respectively. In (b), contour map of peat depth was created using a marching squares algorithm followed by spline interpolation, using the raw data measured at 81 evenly distributed points (coloured dots).

**TABLE 1** Soil (0–40 cm depth) and vegetation properties for the sparse and dense forest areas at the Hälsingfors drained peatland forest.

	Sparse forest	Dense forest
Carbon content (%)	52 ± 1	51 ± 5
Nitrogen content (%)	1.3 ± 0.1	1.7 ± 0.2
CN ratio	42 ± 3	31 ± 3
Mean stem density (stems ha <sup>-1</sup> )	620	1870
Mean stem volume (m <sup>3</sup> ha <sup>-1</sup> )	52	131
Mean tree height (m)	8.7	10.0
Maximum tree height (m)	14.4	18.9
Mean tree diameter (cm)	12.5	10.8
Tree species composition (%)		
<i>Pinus sylvestris</i>	90	7
<i>Picea abies</i>	9	37
<i>Betula pubescens</i>	1	56
Forest floor biomass (g m <sup>-2</sup> )		
Mosses (capitula)	408	231
Dwarf shrubs	269	200
Graminoid	17	0

Note: Tree species composition is based on the number of stems with a diameter at breast height ≥ 40 mm.

inventory conducted in the 12 sample plots during May 2018 indicated that stem density and volume were about two to three times as high in the dense forest than in the sparse forest. The mean (± standard error) soil carbon/nitrogen ratio (CN ratio) over 0–40 cm depth was 42 ± 3 and 31 ± 3 at the sparse and dense forest areas, respectively, based on the soil data sampled at the same 12 sample plots during August 2018. Using an 81-point sampling grid with 50 × 50 m spacing, the estimated peat depth ranged from 10 to 264 cm (mean: 142 ± 13 cm) in the sparse forest and from 12 to 225 cm (mean: 65 ± 7 cm) in the densely forested area. The shallower depths in the dense forest were due to the presence of local moraine ridges (Figure 1b).

The adjacent Hälsingfors natural mire is a topogenous and oligotrophic fen located north of HDPF (Figure 1a). The mire area is dominated by lawns and carpets with short sedges (e.g. *Eriophorum vaginatum*, *Scheuchzeria palustris*, *Trichophorum cespitosum*), and *Sphagnum* mosses (e.g. *Sphagnum papillosum* and *Sphagnum* subg. *Cuspidata*), as well as tall sedges (e.g. *Carex rostrata*) at muddy or loose bottoms (Noumonvi et al., 2023). Woody dwarf shrubs such as *Empetrum nigrum* and *Calluna fuscum* have also been identified on some hummocks. Surficial water flowing through the mire is collected at the mire outlet from where it enters the ditch network of the drained peatland forest area (Figure 1a).

## 2.2 | Measurements of net ecosystem greenhouse gas exchanges and environmental conditions

Continuous measurements of net ecosystem CO<sub>2</sub>, CH<sub>4</sub> and water (H<sub>2</sub>O) exchanges were conducted with the EC method

(Baldocchi, 2003). At the HDPF site, fluctuations of wind and temperature were measured at 10 Hz by a three-dimensional ultrasonic anemometer uSonic-3 Class A anemometer (Metek GmbH, Germany) at 20.2 m height on a telescopic tower located on the border between the sparse and dense forest areas (Figure 1a). Fluctuations of CO<sub>2</sub>, CH<sub>4</sub> and H<sub>2</sub>O concentrations were measured by a closed-path CRDS LGR-FGGA analyser (Model 908-0010; USA). The air inlet was fixed at same height as the anemometer with a horizontal separation of 19 cm. The air was drawn through a polypropylene tubing (Synflex 1300, 2.2 mm inner diameter, 21 m length) by an external pump (Edwards Nxd, UK) into the analyser sample cell at 8 L min<sup>-1</sup>.

The tower at the Hälsingfors mire was equipped with a Metek Usonic-3 Class A anemometer installed at 2.75 m height. The concentrations of CO<sub>2</sub>, H<sub>2</sub>O and CH<sub>4</sub> were measured at 10 Hz with a Picarro G2311-f gas analyser housed within a climate-controlled box. The air intake tube was a custom-made heated intake tube coupled with a Licor rain cap (part number: 9972-072). An auxiliary pump (KNF, Germany) maintained high flow rates (7.5 L min<sup>-1</sup>) to ensure turbulent conditions within the sample tube. The data were digitally streamed from the Picarro to a Campbell CR6 datalogger accounting for digital delays between the two (Fratini et al., 2018). The first 7 months of fluxes at the mire (June 7th 2020 to November 10th 2020) were measured using a CPEC 306 system including a closed-path EC155 for CO<sub>2</sub> and H<sub>2</sub>O analyser (Campbell Scientific, Inc., Logan, UT, USA) and a Licor 7700 analyser (Li-COR Biosciences, USA) for CH<sub>4</sub> flux measurements.

At both sites, the high-frequency EC data were processed with the open-source EddyPro flux calculation software (v7.0.4; Li-COR Biosciences, USA) and averaged into half-hourly CO<sub>2</sub>, CH<sub>4</sub> and H<sub>2</sub>O flux estimates following standard protocols for quality control and corrections. Specifically, double coordinate rotation was used with the three wind velocity components to align the sonic anemometer along the local wind streamlines (Wilczak et al., 2001). Linear trends were removed using block averaging over each 30-min averaging period (Gash & Culf, 1996). Time lags between vertical wind speed and gas concentration were determined by automatic time lag optimization method with a maximum of 30 s searching window (Rebmann et al., 2012). After removing period with low signal strength of EC instruments, the remaining 30-min CO<sub>2</sub>, CH<sub>4</sub> and H<sub>2</sub>O data were then filtered for non-steady state or low turbulent conditions following the quality flags described by Foken et al. (2004). At the forest site, low turbulence conditions were detected and filtered out based on the decoupling of the above and below canopy vertical wind speed (Jocher et al., 2018; Thomas et al., 2013), with the latter continuously measured by an additional ultrasonic anemometer (Adolf Thies GmbH, Germany) installed on a tripod at two metres above the ground. The decoupling threshold values for above and below canopy standard deviation of vertical wind velocity are presented in Figure S1. At the mire, a friction velocity threshold was determined based on the change point detection method (Barr et al., 2013) and applied to filter out data during low turbulent conditions. Statistical outliers defined by any half-hour fluxes that exceeded ± 2 standard

deviations from the 30-day moving window mean for that half-hour were further discarded. At the forest site, the filtered data were then partitioned into sparse and dense forest areas according to wind direction (Figure 1a). After all quality control and filtering steps, 33%, 29% and 42% of all half-hourly  $\text{CO}_2$ ,  $\text{CH}_4$  and  $\text{H}_2\text{O}$  values, respectively, remained for the measurement period. This includes 19%, 17% and 26% of all half-hourly  $\text{CO}_2$ ,  $\text{CH}_4$  and  $\text{H}_2\text{O}$  values from the dense forest area, and 14%, 12% and 16%, respectively, from the sparse forest area (Figure S2). Variations in the data coverage over the measurement period are shown in Figure S2. At the mire, 36%, 50% and 38% of all half-hourly fluxes of  $\text{CO}_2$ ,  $\text{CH}_4$  and  $\text{H}_2\text{O}$  remained, respectively, after the quality control and data filtering procedures.

To obtain annual flux sums, the half-hourly periods with missing  $\text{CO}_2$  and  $\text{H}_2\text{O}$  flux data were filled using the machine learning method called extreme gradient boosting (XGBoost) which was previously recommended in particular for northern flux stations (Kämäräinen et al., 2022; Vekuri et al., 2023). A comparison analysis confirmed that XGBoost outperformed the commonly applied mean diurnal sampling (MDS) method at our study sites (Figures S3 and S4). The XGBoost models were developed using temporal indicators (yearly sine, yearly cosine and decimal day of the year) along with environmental variables including photosynthetic active radiation (PAR), air temperature ( $T_a$ ), soil temperature ( $T_s$ ), relative humidity (RH) and vapor pressure deficit measured at the site (see below). The 10-fold cross validation results indicate reliable performance of the models ( $R^2 = .84-.90$ ; Figure S3), in comparison to the MDS method ( $R^2 = .81-.84$ ; Figure S4). The gap-filled net ecosystem exchange (NEE) was further partitioned into ecosystem respiration ( $R_{\text{eco}}$ ) and gross primary productivity (GPP) using the nighttime-based partitioning method (Reichstein et al., 2005), which was implemented in ReddyProc (Wutzler et al., 2018). The gap-filled GPP was then calculated as the difference between NEE and  $R_{\text{eco}}$ .  $\text{CH}_4$  fluxes from the mire were gap-filled using the random forest machine learning algorithm, as recommended by Irvin et al. (2021). Given that the relatively smaller  $\text{CH}_4$  fluxes in the forest did not strongly correlate with any of the measured environmental variables, gaps were filled with the running average in a 15-day window, centred on the data gap. The uncertainty associated with random measurement errors and gap-filling errors was quantified using Monte Carlo simulations following Richardson and Hollinger (2007).

Water table level and  $T_s$  at 2, 10, 15, 30 and 50 cm depths were continuously recorded with CS451 pressure transducers (Campbell Scientific, Inc.) and TR03 sensors (TOJO Skogsteknik Bygdeå, Sweden), respectively, at four separated soil pits at HDPF (two in each of the sparse and dense forest areas) (Figure 1b) and the adjacent mire (two in hummocks and two in lawns). Ambient  $T_a$  and RH above the tree canopy and at 2 m above the mire surface were continuously measured at the corresponding tower locations with HC2S3 sensor (Campbell Scientific, Inc.). Normalized difference vegetation index (NDVI) was determined from the ratios of reflected over incident radiation at red (640–660 nm) and near-infrared (800–820 nm) spectral bands using a pair of upward and downward looking

spectral reflectance sensors (METER Group, Inc., WA, USA) installed on the top of the towers monitoring the mire and the forest canopies. Midday NDVI was calculated as the average of the readings between 10:00 a.m. and 2:00 p.m. local time (GMT + 1). Net radiation ( $R_n$ ) and its separate in- and outgoing short- and long-wave components were determined with a CNR4 sensor (Campbell Scientific, Inc.). PAR was measured using an Li-190 quantum sensor (Li-Cor, Inc.). At HDPF,  $T_a$ , RH, NDVI,  $R_n$  and PAR were measured both at the flux tower viewing the dense forest area as well as on a meteorological tower within the sparse forest area (Figure 1). Data from these automated sensors were logged on CR1000 data loggers (Campbell Scientific, Inc.) at 1-min intervals and stored as half-hourly averages.

### 2.3 | Manual chamber measurements of forest floor $\text{CO}_2$ and $\text{CH}_4$ exchanges

During the growing seasons of 2020–2022, forest floor  $\text{CO}_2$  and  $\text{CH}_4$  fluxes were measured in each of the 12 sample plots using the closed dynamic chamber method (Livingston & Hutchinson, 1995). Measurements were performed fortnightly during daytime. Permanently installed square aluminium frames (48.5 × 48.5 cm) were inserted 5 cm below the soil surface. The detailed procedures for calculating the net forest floor  $\text{CO}_2$  exchange ( $\text{NE}_{\text{ff}}$ ) and its production (GPP<sub>ff</sub>) and respiration ( $R_{\text{ff}}$ ) components as well as the forest floor  $\text{CH}_4$  exchange are described in the Data S1.

Poor quality flux data, defined by the root-mean-square error (RMSE) and  $r^2$  of the chosen slope of  $dC/dt$ , were filtered out before further analysis. Specifically,  $\text{CO}_2$  fluxes with  $\text{RMSE} > 3.0 \text{ ppm}$  and  $r^2 < .90$ ,  $\text{CH}_4$  fluxes with  $\text{RMSE} > 5.0 \text{ ppb}$  and  $r^2 < .90$ , were removed. These quality control procedures led to the removal of about 4.6% and 8.8% of all measured  $\text{CO}_2$  and  $\text{CH}_4$  fluxes, respectively. Note that the sign convention in this study is such that positive and negative values indicate that the ecosystem is a source and sink, respectively.

Ambient  $T_a$ , chamber headspace  $T_a$ , along with  $T_s$  at 5 and 10 cm depth ( $T_{s5}$ ,  $T_{s10}$ ) outside the frame were recorded manually during each flux measurement using a handheld temperature meter (shaded from direct sunlight during  $T_a$  measurement). PAR was measured with a Hobo® pendant radiation sensor with built-in loggers (Onset Computers, Bourne, MA, USA) and soil moisture within the upper 5 cm (SM) was measured at three sides around the frame during each flux measurement using a GS3 combined moisture–temperature sensor (METER Group, Inc., WA, USA) connected to a ProCheck data logger (METER Group, Inc.). Manual WTL measurements were taken inside PVC groundwater tubes ( $\varnothing = 32 \text{ mm}$  external and 26 mm inside, 125 cm long with 3 mm perforated holes every 2.5 cm) adjacent to each measurement frame and inserted to about 1 m depth into the peat.

It is noteworthy that we also conducted a chamber measurement campaign in August 2020 for quantifying  $\text{N}_2\text{O}$  fluxes at the 12 sampling points in HDPF following the method by Tong et al. (2022). The fluxes were very small with a mean of  $-2.9 \pm 18 \mu\text{g N m}^{-2} \text{ h}^{-1}$  (Figure S5) and equivalent to <1% of the  $\text{CO}_2$  flux in the same period even when

accounting for the 298 higher warming potential of N<sub>2</sub>O relative to CO<sub>2</sub>. Hence, N<sub>2</sub>O emissions from this nutrient-poor ecosystem appeared negligible and were not further considered in this study.

## 2.4 | Aquatic C export via stream discharge

To estimate the aquatic C export, we established three weirs in the study area: one each at the outlets of the ditch network sections that drain the sparse and dense forest areas, and one at the transition between the mire outlet and the inflow of the main drainage ditch (Figure 1a). The rate of aquatic DOC and DIC export was determined by multiplying the discharge flow rate with the concentration of the DOC and DIC. Due to initial issues with leakage at the newly built weirs, and to obtain year-round data, the hourly discharge rate was ultimately determined from continuous recordings of stream water level and established height-discharge rating curves at the nearby (2.6 and 3.1 km north from the mire and forest area, respectively) Degerö Stormyr catchment (C18) using a Parshall flume inside a housed heated shed (Leach et al., 2016). The discharge at C18 was used to estimate the specific discharge in all catchments, which was then multiplied with the annual discharge (Q) estimated with a water balance approach:

$$Q = P - E - S \quad (1)$$

where *P* is rainfall; *E* is the evapotranspiration amount estimated using the gap-filled discharge flux measured at the mire and forest EC towers, the latter of which was further partitioned into sparse and dense forest areas (see Section 2.1); and *S* is the change in water storage calculated by multiplying soil porosity and annual WTL change (*P*, *E* and *S* all in mm). This approach has been widely applied in previous studies conducted in flat landscapes (Ågren et al., 2008).

Concentrations of DOC and DIC were determined regularly resulting in a total of 29 stream water samples collected per weir and hydrological year (i.e. from 1st October to 30th September of the following year), with intensive samplings of 11–12 sampling campaigns occurring during high flow at snow melt flood in April and May. The DOC concentration was quantified using a Shimadzu TOC-CPC analyser (Ågren et al., 2007; Buffam et al., 2007) under the procedure described in Wallin et al. (2011), whereas DIC was determined using a headspace method (Wallin et al., 2013). Previous studies in boreal Swedish surface waters have indicated negligible particulate organic C concentrations relative to the dissolved fraction (Laudon et al., 2011; Leach et al., 2016); thus, the concentration of total organic C was assumed to represent DOC in this study.

## 3 | RESULTS

### 3.1 | Environmental conditions

The magnitudes and seasonal dynamics of PAR were similar during the study period (Figure 2a). During the two hydrological years, the annual mean *T<sub>a</sub>* at the study area was 3.4 and 2.8°C, being slightly

above the long-term (2001–2020) mean of 2.5°C recorded at the nearby ICOS Degerö site (~3.0 km north of HDPF). The daily mean *T<sub>a</sub>* peaked between 22.6 and 23.9°C in July during the three growing seasons (Figure 2b). The mean and maximum *T<sub>s15</sub>* was considerably higher at the mire (mean: 6.2°C; maximum: 19.6°C) than at the sparse (mean: 4.9°C; maximum: 13.7°C) and dense forest areas (mean: 4.6°C; maximum: 12.1°C) over the two hydrological years in HDPF.

The NDVI started to increase in May for both hydrological years and peaked in July over both HDPF and the mire, but the mean midday estimates during the snow-free period of June–October diverged with 0.57, 0.69 and 0.43 in the sparse forest, dense forest and mire, respectively (Figure 2d). In August, early declines of NDVI were observed at the mire compared to HDPF in each of the three growing seasons.

The annual precipitation was 977 and 629 mm for the two hydrological years, the former being significantly above the 20-year average (670 mm), with nearly all of the additional precipitation occurring during June–October (Figure 2c). The dense forest area had the lowest WTL (mean: -32 cm; range: -53 to -12 cm) between May and November, as compared to the sparse forest (mean: -15 cm; range: -32 to +3 cm) and the mire (mean: -6 cm; range: -19 to +9 cm) during the two hydrological years (Figure 2c).

### 3.2 | Seasonal and annual NEE of CO<sub>2</sub> and CH<sub>4</sub>

The NEE measurements extended from March 2020 to September 2022 (Figure 3a; Figure S7a). During this period, HDPF was a net CO<sub>2</sub> sink from April until September, whereas a net emission peak of CO<sub>2</sub> was recorded in October. In the sparse forest, the cumulative annual NEE was -162 ± 10 and -167 ± 11 g C m<sup>-2</sup> year<sup>-1</sup>, while the annual NEE in the dense forest was -98 ± 10 and -138 ± 9 g C m<sup>-2</sup> year<sup>-1</sup> for the two hydrological years, respectively. Maximum mean uptake of -5.3 and -5.1 g C m<sup>-2</sup> day<sup>-1</sup> were recorded in June in the sparse and dense forest, respectively. The mire remained as a net CO<sub>2</sub> sink with a maximum rate of -2.3 g C m<sup>-2</sup> day<sup>-1</sup> during June or July, while during other periods, the NEE remained close to zero except for small emission of 0.32 g C m<sup>-2</sup> day<sup>-1</sup> during autumn (October and November). The annual NEE of the mire was at 2.9 ± 2.0 and -28.4 ± 2.6 g C m<sup>-2</sup> year<sup>-1</sup> for the two hydrological years.

Based on the plot-scale chamber data averaged over all growing seasons, the instantaneous daytime forest floor net CO<sub>2</sub> exchange (NE<sub>ff</sub>) resulted in a sink of -29 ± 6 and a source of 91 ± 6 mg C m<sup>-2</sup> h<sup>-1</sup> in the sparse and dense forest areas, respectively (Figure 4). Similarly, the forest floor GPP (GPP<sub>ff</sub>) was about three times greater in the sparse forest (-130 ± 8 mg C m<sup>-2</sup> h<sup>-1</sup>) than in the dense forest area (-39 ± 5 mg C m<sup>-2</sup> h<sup>-1</sup>). Meanwhile, forest floor respiration (*R<sub>ff</sub>*) was higher at the dense forest (130 ± 5 mg C m<sup>-2</sup> h<sup>-1</sup>) than at the sparse forest area (100 ± 5 mg C m<sup>-2</sup> h<sup>-1</sup>).

Hälsingfors drained peatland forest was a small CH<sub>4</sub> source during almost the entire measurement period, with flux magnitudes ranging from -4.8 to 11.5 mg C m<sup>-2</sup> day<sup>-1</sup> (Figure 3b; Figure S7b).

**FIGURE 2** Daily means for environmental variables including (a) photosynthetically active radiation (PAR), (b) air ( $T_a$ ) and soil temperature ( $T_s$ ) at the 15 cm depth, (c) water table level (WTL) with daily precipitation in the study areas, (d) normalized difference vegetation index (NDVI) and (e) 15-day running mean of evapotranspiration (ET) during the study period (including the two hydrological years indicated on top). NDVI and WTL data are presented during the snow-free season. Environmental conditions during manual chamber measurements are presented in Figure S6.

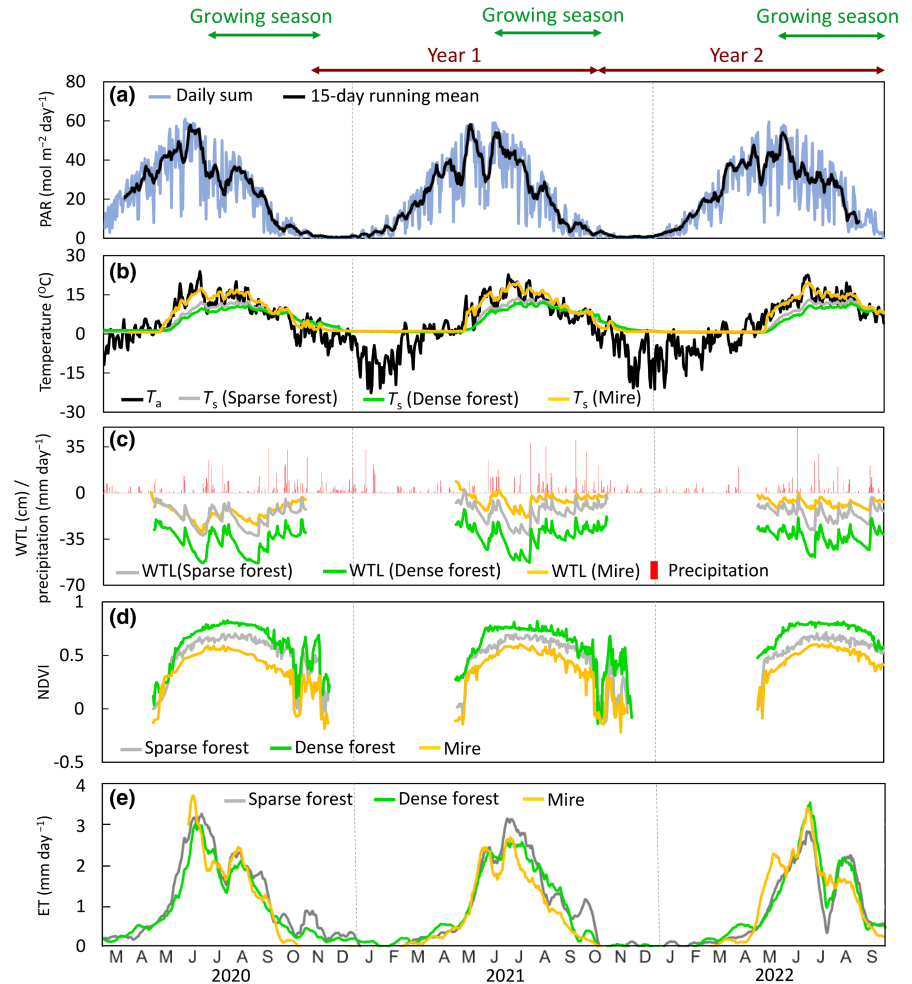
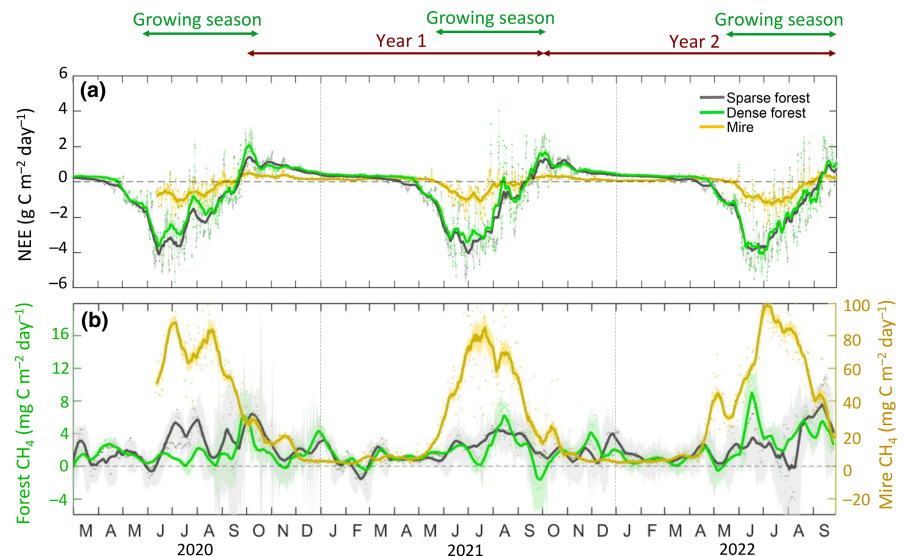


**FIGURE 3** Daily sums of (a) net ecosystem  $\text{CO}_2$  exchange (NEE) and (b) methane ( $\text{CH}_4$ ) fluxes for Hälsingfors drained peatland forest (partitioned into both sparse and dense forest areas) and the adjacent mire from March 2020 to September 2022 (including the two hydrological years). The shade areas represent the standard deviation of daily fluxes, while the bold dark lines denote the 15-day running means. In (b),  $\text{CH}_4$  fluxes from the forest and mire refer to the left and right axis, respectively.



Emission peaks coincided in general with rainfall events which led to subsequent increase in WTL. Except during June and July 2020 when the  $\text{CH}_4$  emission in the sparse forest was about three times as high as in the dense forest, no significant difference (independent sample  $t$ -test  $p > .05$ ) in the gap-filled ecosystem  $\text{CH}_4$  emission was

noted between the two contrasting forest areas. Averaged over the two hydrological years, the sparse and dense forest areas were small annual sources of  $\text{CH}_4$  with  $0.76 \pm 0.06$  and  $0.71 \pm 0.05 \text{ g C m}^{-2} \text{ year}^{-1}$ , respectively (Table 2). The plot-scale chamber data suggested on average higher forest floor  $\text{CH}_4$  emission of  $0.71 \pm 0.05 \text{ mg C m}^{-2} \text{ h}^{-1}$

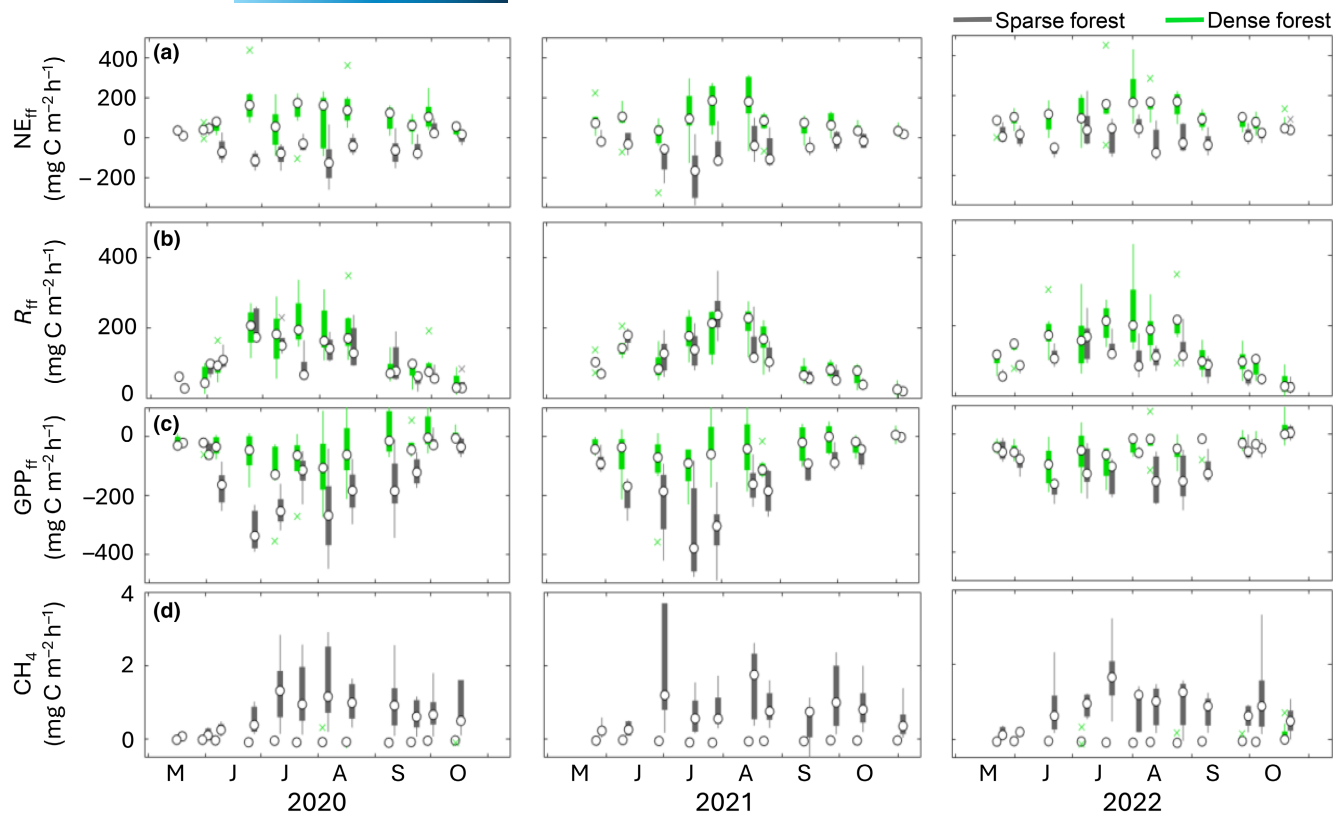


**FIGURE 4** Seasonal variations in forest floor fluxes of (a–c) carbon dioxide ( $\text{CO}_2$ ) and (d) methane ( $\text{CH}_4$ ) measured with manual chambers in the Hälsingfors drained peatland forest area during the growing seasons of 2020–2022.  $\text{CO}_2$  fluxes include the forest floor (a) net  $\text{CO}_2$  exchange ( $\text{NE}_{\text{ff}}$ ), (b) respiration ( $R_{\text{ff}}$ ) and (c) gross primary productivity ( $\text{GPP}_{\text{ff}}$ ). Positive and negative values represent losses and uptake by the ecosystem, respectively. The circles denote sample ( $n=5$  and  $7$  in the sparse and dense forest areas, respectively) medians, while the bars and whiskers denote the interquartile range and total range. Outliers (crosses) are defined as the values  $>1.5$  interquartile range.

in the sparse forest compared to a close-to-neutral  $\text{CH}_4$  flux of  $-0.05 \pm 0.01 \text{ mg C m}^{-2} \text{ h}^{-1}$  in the dense forest (Figure 4d).

There was a clear seasonal pattern in the mire where  $\text{CH}_4$  emissions reached up to  $100 \text{ mg C CH}_4 \text{ m}^{-2} \text{ day}^{-1}$  and peaked during the summer (June to August) (Figure 3b), following the temporal dynamics of  $T_a$  and vegetation growth (Figure 2). The annual ecosystem-scale  $\text{CH}_4$  emission from the mire was on average  $9.8 \pm 0.1 \text{ g C m}^{-2} \text{ year}^{-1}$  (Table 2), being about 13 times as high as in the drained peatland forest. Averaged over three summers (June–August), the  $\text{CH}_4$  emission from the mire was 27 times as much as from the forest area. Relative to the mire site, no clear pattern of seasonality was observed in the forest site.

### 3.3 | Environmental responses of ecosystem $\text{CO}_2$ and $\text{CH}_4$ fluxes

The relationship between air temperature and measured  $R_{\text{eco}}$ , defined as the filtered half-hourly fluxes during nighttime (i.e.  $\text{PAR} < 10 \mu\text{mol m}^{-2} \text{ s}^{-1}$ ), differed among the forest area and mire sites (Figure 5a; Table S1). Specifically, the parameter of basal respiration at  $10^\circ\text{C}$  (i.e.  $R_{10}$ ) was significantly (independent sample  $t$ -test  $p < .05$ ) higher at the forest sites ( $2.92$  and  $3.17 \mu\text{mol m}^{-2} \text{ s}^{-1}$  at sparse

and dense areas, respectively) than in the mire ( $1.04 \mu\text{mol m}^{-2} \text{ s}^{-1}$ ). The air temperature sensitivity parameter ( $E_0$ ) was significantly lower at the forest sites ( $220$  and  $256^\circ\text{C}^{-1}$  at sparse and dense areas, respectively) than at the mire site ( $312^\circ\text{C}^{-1}$ ). The  $R_{10}$  and  $E_0$  of the forest floor were higher and lower in the sparse forest area ( $R_{10} = 1.80 \mu\text{mol m}^{-2} \text{ s}^{-1}$ ;  $E_0 = 215$ ) than in the dense area ( $R_{10} = 2.59 \mu\text{mol m}^{-2} \text{ s}^{-1}$ ;  $E_0 = 153^\circ\text{C}^{-1}$ ), respectively, resulting altogether in a greater  $R_{\text{ff}}$  in the dense area at any temperature during the growing season.

The light response of half-hourly GPP derived as the difference of measured daytime NEE and modelled  $R_{\text{eco}}$ , varied across the sites. Specifically, the light response parameters  $\alpha$  and  $P_{\text{max}}$ , which represent the initial quantum yield efficiency ( $\alpha$ ) and maximum ecosystem photosynthetic rate at light saturation ( $P_{\text{max}}$ ), respectively, were about four to six times as high as at the forest compared to the mire (Figure 5b; Table S1). Between the two different forest areas, both ecosystem and forest floor  $\alpha$  were significantly smaller ( $p < .05$ ) at the dense forest, respectively, compared to the sparse forest. Furthermore, ecosystem  $P_{\text{max}}$  was similar in the sparse and dense forest whereas  $P_{\text{max}}$  of the forest floor was significantly greater ( $p < .05$ ) in the sparse area. This resulted altogether in greater  $\text{GPP}_{\text{ff}}$  in the sparse forest area at any light level during the growing season, compared to the dense forest area.



**TABLE 2** Annual net ecosystem carbon balance (NECB) and its component fluxes including net ecosystem CO<sub>2</sub> exchange (NEE) measured by eddy covariance, that is, the balance of ecosystem respiration ( $R_{\text{eco}}$ ) and gross primary productivity (GPP), net ecosystem methane (CH<sub>4</sub>) exchange measured by eddy covariance and the lateral aquatic export of dissolved organic (DOC) and inorganic (DIC) carbon at the Hälsingfors drained peatland forest site (HDPF; for the total area and when partitioned into the sparse and dense forest areas) and the adjacent mire during the hydrological years 2020–2021 and 2021–2022.

	HDPF			
	Sparse forest	Dense forest	Total area	Mire
NEE	2020–2021	2020–2021	2020–2021	2020–2021
	2021–2022	2021–2022	2021–2022	2021–2022
	(g C m <sup>-2</sup> year <sup>-1</sup> )	(g C m <sup>-2</sup> year <sup>-1</sup> )	(g C m <sup>-2</sup> year <sup>-1</sup> )	(g C m <sup>-2</sup> year <sup>-1</sup> )
NEE	-162 ± 10	-98 ± 10	-126 ± 6	2.9 ± 2.0
$R_{\text{eco}}$	-167 ± 11	-138 ± 9	-143 ± 5	-28.4 ± 2.6
	758 ± 25	785 ± 33	773 ± 20	278 ± 7
GPP	722 ± 33	746 ± 35	737 ± 22	260 ± 7
	-920 ± 27	-883 ± 32	-899 ± 21	-275 ± 6
CH <sub>4</sub>	-889 ± 35	-884 ± 35	-880 ± 23	-288 ± 6
	0.76 ± 0.08	0.63 ± 0.07	0.71 ± 0.05	9.0 ± 0.1
DOC	0.76 ± 0.08	0.79 ± 0.07	0.78 ± 0.05	10.6 ± 0.1
	10.5 ± 1.3	23.0 ± 2.5	18.3 ± 2.1 <sup>a</sup>	13.6 ± 1.7
DIC	9.4 ± 1.2	19.6 ± 2.5	15.7 ± 2.1 <sup>a</sup>	13.2 ± 1.6
	1.2 ± 0.1	1.6 ± 0.2	1.5 ± 0.1 <sup>a</sup>	4.0 ± 0.5
NECB	1.2 ± 0.1	1.6 ± 0.2	1.5 ± 0.1 <sup>a</sup>	4.2 ± 0.6
	-150 ± 10	-73 ± 10	-105 ± 6	29.5 ± 2.7
	-156 ± 11	-116 ± 9	-125 ± 6	-0.4 ± 3.1

Note: Annual estimates are presented with ±1 standard deviation based on the Monte Carlo uncertainty analysis.

<sup>a</sup>Total area lateral DOC and DIC fluxes in HDPF were calculated by the area-weighted average between sparse and dense forest estimates.

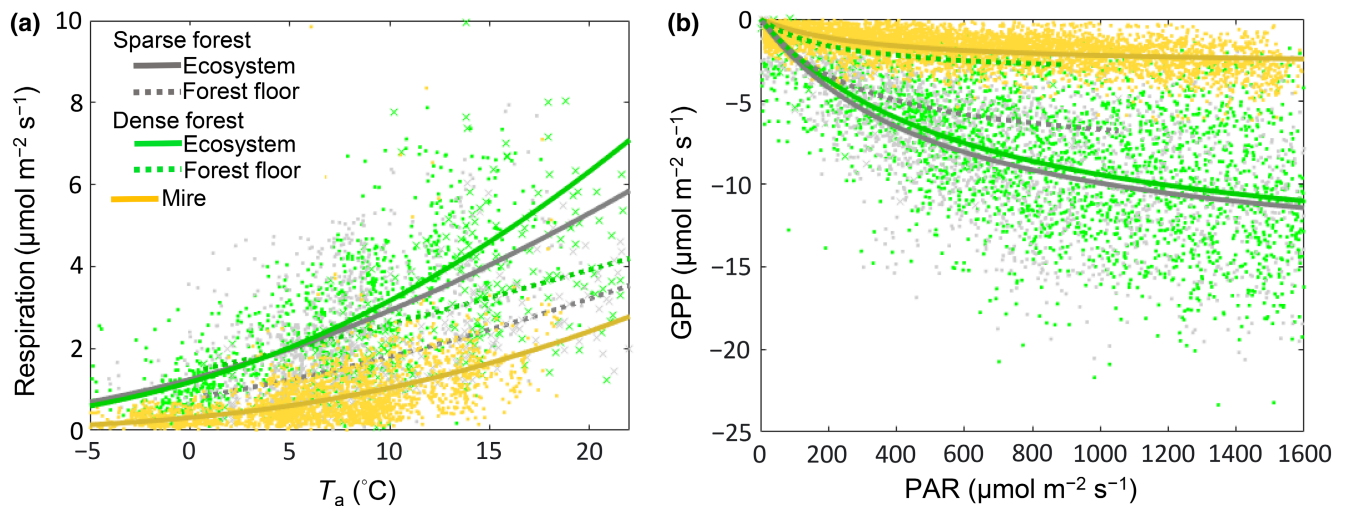


**FIGURE 5** Response of half-hourly (symbols) ecosystem and forest floor (a) respiration to air temperature ( $T_a$ ) and (b) gross primary productivity (GPP) to photosynthetically active radiation (PAR) during the snow-free periods for the sparse and dense forest and mire sites. Solid and dotted lines represent the fit lines for the ecosystem and forest floor, respectively. The model equations and parameters for the fit lines are presented in Table S1.

Mire CH<sub>4</sub> emissions were <10 mg C m<sup>-2</sup> day<sup>-1</sup> under flooded conditions during early spring and late autumn but increased to >100 mg C m<sup>-2</sup> day<sup>-1</sup> with decreasing WTL during the growing season (Figure 6). Comparatively, the CH<sub>4</sub> fluxes from the forests were consistently <10 mg C m<sup>-2</sup> day<sup>-1</sup> independent of WTL changes. Within the same WTL range of -10 to -20 cm, the mire emitted on average about 20 times more CH<sub>4</sub> than the sparse forest area.

### 3.4 | Aquatic C export from the catchment

The seasonal variation of the dissolved C (DC) export was primarily driven by the discharge pattern. More than 50% of the DC export was generated during the spring season, with another 40% associated with the rainfall events during the growing season (Figure 7). In comparison, the seasonal variation of DC concentration was

relatively smaller than that of discharge rate. The peak of DC concentration was typically observed in August and September, followed by a decline towards winter.

Annual aquatic C export differed between the sparse and dense forest areas within HDPF. Averaged over the two hydrological years, the annual DC export from the sparse forest was  $11.1 \pm 1.0 \text{ g C m}^{-2} \text{ year}^{-1}$  (Table 2). In comparison, the annual DC export in the dense forest was more than two times higher, being  $22.9 \pm 2.0 \text{ g C m}^{-2} \text{ year}^{-1}$ . In both areas, the DOC export contributed about 90% to total annual DC (DOC:DIC=8:1 in sparse forest and 13:1 in dense forest). The DOC and DIC concentrations were 125%

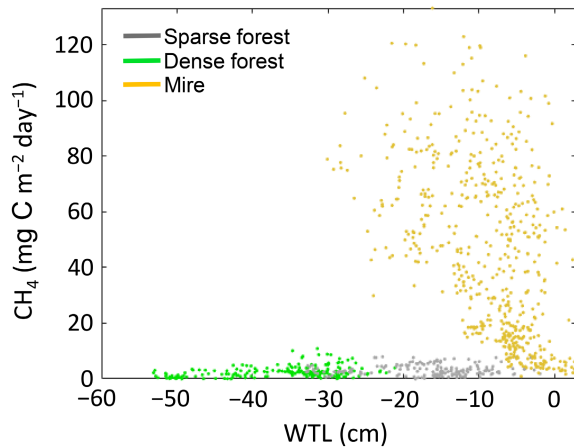


**FIGURE 6** Relationships between daily mean water table level (WTL) and methane ( $\text{CH}_4$ ) flux based on eddy covariance measurements at the Hälsingfors drained peatland forest (shown separately for the sparse and dense forest areas) and mire sites during the growing seasons of 2020–2022.

and 60% higher at the dense forest compared to the sparse forest in the stream water samples. The annual DOC export from the mire of  $13.3 \pm 1.7 \text{ g C m}^{-2} \text{ year}^{-1}$  was in between the sparse and dense forest sites, whereas the DIC export from the mire of  $4.1 \pm 0.4 \text{ g C m}^{-2} \text{ year}^{-1}$  was three and two times higher than in the sparse and dense forest areas, respectively, averaged over the two hydrological years (Table 2). Combined, the total aquatic C export from the mire was  $14.3 \pm 1.4 \text{ g C m}^{-2} \text{ year}^{-1}$  in 2020–2021 and  $15.0 \pm 1.5 \text{ g C m}^{-2} \text{ year}^{-1}$  in 2021–2022, with an annual mean DOC:DIC ratio of 7:1 (Figure 7).

### 3.5 | The net ecosystem C balance

By integrating the terrestrial and aquatic C flux components, we estimated the NECB of the boreal peatland forest to be a net C sink with an average of  $-115 \pm 5 \text{ g C m}^{-2} \text{ year}^{-1}$  over the two hydrological years. The C sink strength of  $-153 \pm 8 \text{ g C m}^{-2} \text{ year}^{-1}$  of the sparse forest area was 61% larger in comparison to  $-95 \pm 8 \text{ g C m}^{-2} \text{ year}^{-1}$  in the dense forest area (Table 2). At both the sparse and dense forest, the NECB was dominated by NEE while  $\text{CH}_4$  emissions and DC export contributed <1% and about 14%, respectively (Table 2).

The adjacent mire had a positive NECB of  $14.6 \pm 1.7 \text{ g C m}^{-2} \text{ year}^{-1}$  averaged over the two hydrological years. The uptake of C via NEE of  $-12.8 \pm 1.6 \text{ g C m}^{-2} \text{ year}^{-1}$  was counterbalanced by the  $\text{CH}_4$  emission ( $9.8 \pm 0.1 \text{ g C m}^{-2} \text{ year}^{-1}$ ) and aquatic DC export ( $17.5 \pm 1.5 \text{ g C m}^{-2} \text{ year}^{-1}$ ). While the NEE of  $\text{CO}_2$  and  $\text{CH}_4$  contributed about equally and together dominated (>93%) to the NECB between June and September, aquatic DOC and DIC contributed 42% to the mire NECB during the high discharge periods in spring (April) and autumn (October and November).

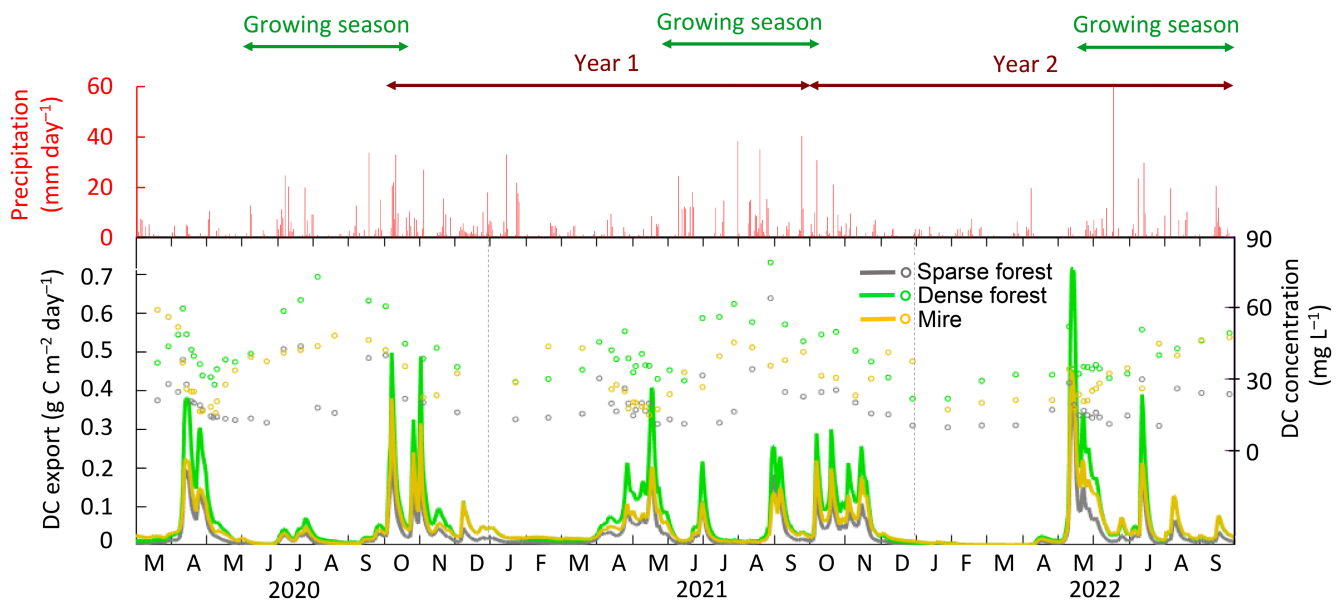


**FIGURE 7** Daily sums of precipitation (top panel) and total dissolved carbon (DC; including organic and inorganic C) export (bottom panel) at the Hälsingfors drained peatland forest (for the total area and partitioned into the sparse and dense forest areas) and the adjacent mire from March 2020 to September 2022 (including the two hydrological years). In the bottom panel, solid lines denote DC export (left axis), whereas circular symbols denote concentration of DC from manually collected samples.

## 4 | DISCUSSION

### 4.1 | A boreal nutrient-poor peatland forest acts as a net ecosystem C sink

This study integrated terrestrial and aquatic C fluxes into annual ecosystem-scale C balances for a typical boreal peatland forest and an adjacent mire over two hydrological years. Our main finding that this >100-year-old drained nutrient-poor peatland forest was a net C sink ( $-105$  to  $-125\text{ g C m}^{-2}\text{ year}^{-1}$ ), suggests that not all of the historically drained peatland forests act today as C sources. In fact, previous studies reporting boreal peatland forests as significant C sources were either conducted on a forest established on former agricultural land with nutrient-rich soils (CN ratio = 13–28, Lohila et al., 2007), or accounted for additional C losses due to thinning and harvest activities (He et al., 2016; Kasimir et al., 2018). It is noteworthy, however, that also nutrient-rich peatland forests (CN ratio = 23–27) may act as small contemporary C sink of  $-20$  to  $-70\text{ g C m}^{-2}\text{ year}^{-1}$  at the ecosystem scale (Korkiakoski et al., 2023; Meyer et al., 2013). Compared to our site, nutrient-poor peatland forests (CN ratio = 34–90) in southern boreal Finland may provide even greater net  $\text{CO}_2$  sinks in the range of  $-234$  to  $-570\text{ g C m}^{-2}\text{ year}^{-1}$  (Laine et al., 1996; Lohila et al., 2011; Minkkinen et al., 2018). Altogether, this indicates that the ecosystem C sink-source strength of drained peatland forests strongly depends on nutrient availability, with climate being a secondary modifier. It is further noteworthy that the C sink strength of nutrient-poor peatland forests may be close to that of boreal upland mineral forests (Anderson-Teixeira et al., 2021; Lindroth et al., 2020). Given that nutrient-poor regions dominate the land area in Fennoscandia (e.g. 72% in Sweden with CN ratio >30 in organic forest soils, Olsson, 1999), drained peatland forests in those regions may presently provide an important contribution to climate change mitigation. It is further important to note that while our study explored the ecosystem-scale C balance, it does not provide information on whether the peat layer itself is acting as a C sink or source, the latter being critical for understanding the long-term climate impact of these forested ecosystems. Previous studies, however, have reported that, in contrast to the significant C losses observed in nutrient-rich peat (He et al., 2016; Kasimir et al., 2018), the peat layer in nutrient-poor boreal peatland forests may act as small C sinks (Ojanen et al., 2013).

The observation that our drained peatland forest acted as a source of  $\text{CH}_4$  contrasts previous studies suggesting that drained peatland forests with mean WTL  $\leq -30$  cm act as  $\text{CH}_4$  sink (Korkiakoski et al., 2017; Minkkinen et al., 2007; Ojanen et al., 2010). This could be explained by the relatively high WTL at the sparse forest section (mean WTL =  $-15$  cm) and the existence of locally flooded areas in the dense forest section (mean WTL =  $-32$  cm). In addition, while previous estimates relate to soil  $\text{CH}_4$  fluxes, our continuous (half-hourly) and ecosystem-scale measurements might have captured spatiotemporal peaks and emissions via trees (Ranniku et al., 2023; Vainio et al., 2022) and from ditches (Peacock et al., 2021). Overall, our results suggest a negligible contribution of the  $\text{CH}_4$  flux to the

annual NECB and GHG balance (accounting for its 28 times higher warming potential over a 100-year time frame; IPCC, 2022) in our drained boreal peatland forest.

The aquatic DOC ( $17.0\text{ g C m}^{-2}\text{ year}^{-1}$ ) and DIC ( $1.5\text{ g C m}^{-2}\text{ year}^{-1}$ ) fluxes in HDPF are higher or at the high end, respectively, when compared to other boreal stream networks in the surrounding boreal forest landscape (DOC:  $6.1$ – $9.9\text{ g C m}^{-2}\text{ year}^{-1}$ ; DIC:  $-0.7$ – $1.5\text{ g C m}^{-2}\text{ year}^{-1}$ ) (Ågren et al., 2007; Wallin et al., 2010). In contrast to the minor role of the  $\text{CH}_4$  flux, the aquatic C export could offset about 14% of the terrestrial C sink in our boreal peatland forest. In comparison, an average offset of 9% and 32% has been reported for boreal upland forests (Webb et al., 2019) and natural peatlands (Nilsson et al., 2008), respectively. It is furthermore noteworthy that the C sink reduction by aquatic C losses differed with 8% and 20% between the sparse and dense forest areas which indicate the potential for a high spatially varying contribution of aquatic C fluxes to NECB. Overall, these results highlight the important role of aquatic C fluxes and the need for their accounting in estimates of the ecosystem C balance of drained peatland forests.

The peatland forest was a stronger annual C sink than the adjacent mire, which was close to C neutral. However, earlier findings from the nearby ( $\sim 3$  km) Degerö mire suggested an NECB of  $-20$  to  $-27\text{ g C m}^{-2}\text{ year}^{-1}$  in 2004 and 2005 (Nilsson et al., 2008). The primary cause for this between-mire difference is that the annual net  $\text{CO}_2$  uptake ( $-12.8 \pm 1.6\text{ g C m}^{-2}\text{ year}^{-1}$ ) from the Hälsingfors mire was less than at the Degerö mire ( $-58 \pm 21\text{ g C m}^{-2}\text{ year}^{-1}$ ; Nilsson et al., 2008; Peichl et al., 2014). One explanation could be the presence of large areas of mud-bottom flarks (or algal pools) at the Hälsingfors mire, which are not found at the Degerö mire. These seasonally inundated pools are typical of aapa mires in sub-arctic Fennoscandia. It has long been speculated that such areas were a source of carbon (e.g. Sallinen et al., 2023; Sjörs, 1990) and footprint analysis carried out on our EC data appears to confirm these as a source of  $\text{CO}_2$  (Noumonvi et al., 2023). Nevertheless, it is important to note that the present-day comparison of NECB between natural and drained peatlands does not reflect their long-term climate impact. Specifically, whereas the relatively smaller mire C sink may persist over centuries (e.g. Frolking et al., 2011), drained peatland forests might become C sources in the long run if the peat soil remains as a C source after the accounting for the removal of C stored in tree biomass via tree harvest (He et al., 2016; Kasimir et al., 2018). The long-term C balance of drained peatland forest will further depend on the use of extracted biomass for short- versus long-lived wood products and for substituting fossil fuel emissions (Leskinen et al., 2018; Skogsstyrelsen, 2021).

The potential of boreal peatland forests to act as present-day C sink has implications for developing management strategies, which aim at sustainable and climate-smart timber production while ensuring the provision of other ecosystem services. For instance, the current interest in the rewetting of drained peatland forests should consider local conditions (i.e. site fertility and climate) and primarily target nutrient-rich sites, as rewetting of nutrient-poor peatland forest may result in limited climate benefits (Ojanen &

Minkinen, 2020). In comparison, active forestry may maintain tree C uptake; however, biomass removal via harvest might in the long-term result in a net C loss (He et al., 2016; Kasimir et al., 2018). Alternatively, low-productive and economically low-interest areas as resembled by our sparse forest site could constitute important long-term C sinks when set aside from active forestry. However, since further supporting data from drained peatland forests are currently missing particularly in middle and northern boreal regions, caution is needed when extrapolating results from single-site studies and considerably more information will be needed to improve our understanding of present-day climate-forcing effects from historic drainage activities in Fennoscandia.

## 4.2 | Environmental responses of NECB components differ between peatland forest and mire

The different temperature and light sensitivity of  $R_{\text{eco}}$  and GPP, respectively, between HDPF and the nearby mire suggest that long-term drainage has altered the response of the  $\text{CO}_2$  exchanges to these key environmental controls. Specifically, the lower sensitivity of  $R_{\text{eco}}$  to  $T_a$  in HDPF ( $E_0 = 220$  and  $256^\circ\text{C}^{-1}$  in sparse and dense areas, respectively) than the mire ( $E_0 = 312^\circ\text{C}^{-1}$ ) implies that future warming will likely have less impact on the respiratory C losses from drained forests compared to natural peatlands (Ratcliffe et al., 2017). Meanwhile, the greater photosynthetic capacity at HDPF could be attributed to the additional contribution of the tree layer relative to the mire. Thus, our study demonstrates that peatland drainage may alter the environmental controls of  $\text{CO}_2$  fluxes and subsequently the response of the NECB to future climatic changes.

Even though  $\text{CH}_4$  emission peaks appeared to coincide with rainfall events, we noted a remarkable lack of significant relationships between  $\text{CH}_4$  emission with WTL or  $T_s$  which might be explained by their limited seasonal variations. The lower seasonal variability of  $T_s$  in the forest area is likely due to forest canopy shading (Hedwall et al., 2015), whereas a disconnection between water table and surface moisture due to capillary action of peat and mosses may dampen the effects of WTL fluctuations (Lafleur et al., 2005; Ratcliffe et al., 2019). In contrast, we observed a negative relationship suggesting increasing  $\text{CH}_4$  flux under decreasing WTL at the mire. This appears counterintuitive but might result from the over-riding effects from higher  $T_s$  and vegetation biomass on  $\text{CH}_4$  production during the warmer and drier summer period (Moosavi & Crill, 1997; Treat et al., 2007). It is further noteworthy that, at given WTL and  $T_s$ , substantially lower  $\text{CH}_4$  emissions occurred in the drained forest compared to the mire. This suggests that long-term drainage reduced the activity of the methanogenic bacteria and/or enhanced the activity of methanotrophic bacteria due to increased peat aeration (Yrjälä et al., 2011). Thus, long-term drainage may not only change the hydrological conditions but also create a substantial divergence in associated  $\text{CH}_4$  dynamics.

The contrasting annual DC export between the peatland forest and mire sites was controlled by differences in DOC concentrations

rather than by those in DIC concentration or discharge rate. The high stream DOC concentration particularly at the dense forest might reflect the greater amount and higher quality of the organic matter input from the tree canopy. Similarly, Nieminen et al. (2021) observed higher DOC concentrations in various Fennoscandian drained peatlands compared to mires. It is, however, notable that they report substantial drainage effects on DOC concentrations only in southern boreal regions, whereas limited impacts were noted in northern boreal regions. Thus, while drainage may alter stream C concentrations, annual C export rates might be further modified in response to climatic factors.

## 4.3 | Forest structure may act as a key control on NECB in the drained peatland forest

Our results revealed a considerable difference of individual forest NECB components among the two distinct forest sections. While our study design is lacking the replication needed for disentangling the role of the various forest structure elements as potential drivers, this finding indicates that contrasting forest structure may considerably regulate the NECB. Specifically, the sparse pine-dominated forest characterized by a lower tree density was a stronger C sink (mainly due to a difference in NEE) compared to the dense forest area. While this result appears counterintuitive at first, we found that larger net  $\text{CO}_2$  uptake by the forest floor in the sparse area may explain the enhanced ecosystem-scale C sink. This was a result of both lower respiration (i.e.  $R_{\text{ff}}$ ) and a greater  $\text{GPP}_{\text{ff}}$  response to light in the sparse area. In addition, given the reduced tree cover, higher amounts of solar radiation reaching the sparse forest floor (Figure S4) further enhanced ground vegetation GPP in the sparse forest area. Considerable contributions of *Sphagnum*-dominated ground vegetation to the ecosystem C balance of boreal peatland forests have been previously noted (Kasimir et al., 2021; Kulmala et al., 2019). The lower  $R_{\text{ff}}$  is likely due to the higher WTL in the sparse forest. However, the relative difference in  $R_{\text{ff}}$  was less compared to that in  $\text{GPP}_{\text{ff}}$ . Thus, our results further highlight the important role of the tree-understory vegetation composition in regulating the spatial heterogeneity in the NECB of drained boreal peatland forests.

The different sensitivity of  $\text{CO}_2$  fluxes to environmental factors in the two forest areas further demonstrates the role of forest structure in regulating the net  $\text{CO}_2$  exchange. Specifically, in the birch-dominated dense forest, the delayed GPP onset relative to the sparse forest might reflect strategies of deciduous trees to avoid frost damage to new leaves (Cannell & Smith, 1986; Welp et al., 2007). The higher temperature sensitivity of  $R_{\text{eco}}$  at the dense forest likely explains its smaller net  $\text{CO}_2$  uptake compared to sparse forests in warm periods. While the higher temperature response of  $R_{\text{eco}}$  corresponds to greater tree biomass, the lower CN ratio in the dense forest area might also result in increased microbial peat decomposition, particularly at higher temperatures

(Mao et al., 2018). Overall, this highlights the potential of diverging effects from warming on the spatial and temporal variations of CO<sub>2</sub> fluxes and subsequently on the NECB of drained peatland forests. However, given that the data coverage after separating into sparse and dense forest area was relatively limited, our results on detailed effects of forest structure on C fluxes should be treated with some caution.

It is further noteworthy that we observed inconsistencies between our EC- and chamber-derived estimates of CH<sub>4</sub> fluxes with respect to the relative difference between the two forest areas. Specifically, chamber-derived CH<sub>4</sub> emissions were significantly lower and higher in the sparse and dense forest areas, respectively, compared to EC estimates. The mismatch in the dense forest might arise from local flooded areas with higher CH<sub>4</sub> emissions as well as additional emissions from tree stems (Ranniku et al., 2023; Vainio et al., 2022) and ditches (Peacock et al., 2021), all of which were not captured by chamber measurements. In the sparse forest, the higher chamber CH<sub>4</sub> emission estimate was driven by large fluxes from three of the five sampling locations (Figure S8). While these hotspots contributed substantially to chamber fluxes, they might constitute a relatively small portion of the EC footprint area.

Given similar soil C content at the two forest areas, the higher stream C export and twofold higher DOC concentrations at the dense compared to sparse forest areas might be explained by the difference in tree biomass. Greater amounts of litterfall and contribution from easily degradable birch litter (Figure S9) combined with the absence of slow decomposing *Sphagnum* litter support the greater stream C input at the dense forest. This result is in line with Nieminen et al. (2021) who reported a positive correlation between stand volume and DOC concentrations across 71 drained boreal peatland forest sites. Litterfall and exudates have further been shown to be correlated positively with DOC export in Norwegian forest ecosystems (Finstad et al., 2016). Altogether, this highlights that forest structure, that is, primarily differences in stand volume and species composition, may act as a key factor in regulating the aquatic C export from drained boreal peatland forests.

## AUTHOR CONTRIBUTIONS

**Cheuk Hei Marcus Tong:** Conceptualization; data curation; formal analysis; investigation; methodology; software; validation; visualization; writing – original draft. **Koffi Dodji Noumonvi:** Data curation; methodology; software; validation; writing – review and editing. **Joshua Ratcliffe:** Data curation; software; validation; writing – review and editing. **Hjalmar Laudon:** Methodology; resources; writing – review and editing. **Järvi Järveoja:** Writing – review and editing. **Andreas Drott:** Supervision; writing – review and editing. **Mats B. Nilsson:** Project administration; resources; supervision; writing – review and editing. **Matthias Peichl:** Conceptualization; funding acquisition; methodology; project administration; resources; supervision; writing – original draft; writing – review and editing.

## ACKNOWLEDGEMENTS

This study was funded by the Swedish Research Council for Environment, Agricultural Sciences and Spatial Planning (FORMAS) (grants #2016-01289 and #2020-01446) and the Stiftelsen Oscar och Lili Lamms Minne Foundation (grant #2017.4.1-68). Additional funding from the Knut and Alice Wallenberg Foundation (grant #2018.0259) and financial support from the Swedish Research Council and consortium partners to the Swedish Infrastructure for Ecosystem Science (SITES, grant #2017-00635) is also acknowledged. The instrumentation at the Hälsingfors mire was financed by infrastructure grants from the Kempe Foundations (grant #JCK-1712) and the Swedish University of Agricultural Sciences (SLU). We thank the land owners Vivan Andersson and the state-owned forest company Sveaskog for allowing this research to be carried out at the Hälsingfors forest and mire sites, respectively. We also thank the engineers and technicians from the SLU Unit for Field-based Forest Research for maintenance and operation of equipment and experiments at the Kulbäcksliden Research Infrastructure.

## CONFLICT OF INTEREST STATEMENT

The authors declare that the research was conducted in the absence of any commercial or financial relationships that could be construed as a potential conflict of interest.

## DATA AVAILABILITY STATEMENT

The data that support the findings of this study are openly available in Dryad at <http://doi.org/10.5061/dryad.gqnk98sw5>.

## ORCID

Cheuk Hei Marcus Tong  <https://orcid.org/0000-0002-8805-4040>

Järvi Järveoja  <https://orcid.org/0000-0001-6317-660X>

Mats B. Nilsson  <https://orcid.org/0000-0003-3765-6399>

Matthias Peichl  <https://orcid.org/0000-0002-9940-5846>

## REFERENCES

- Ågren, A., Berggren, M., Laudon, H., & Jansson, M. (2008). Terrestrial export of highly bioavailable carbon from small boreal catchments in spring floods. *Freshwater Biology*, 53(5), 964–972. <https://doi.org/10.1111/j.1365-2427.2008.01955.x>
- Ågren, A., Buffam, I., Jansson, M., & Laudon, H. (2007). Importance of seasonality and small streams for the landscape regulation of dissolved organic carbon export. *Journal of Geophysical Research: Biogeosciences*, 112(G3), 381. <https://doi.org/10.1029/2006JG000381>
- Ahti, T., Hämet-Ahti, L., & Jalas, J. (1968). Vegetation zones and their sections in northwestern Europe. *Annales Botanici Fennici*, 5, 169–211.
- Alm, J., Shurpali, N. J., Minkinen, K., Aro, L., Hytönen, J., Laurila, T., Lohila, A., Maljanen, M., Martikainen, P. J., Mäkiranta, P., Penttälä, T., Saarnio, S., Silvan, N., Tuittila, E.-S., & Laine, J. (2007). Emission factors and their uncertainty for the exchange of CO<sub>2</sub>, CH<sub>4</sub> and N<sub>2</sub>O in Finnish managed peatlands. *Boreal Environment Research*, 12, 191–209.
- Anderson-Teixeira, K. J., Herrmann, V., Morgan, R. B., Bond-Lamberty, B., Cook-Patton, S. C., Ferson, A. E., Muller-Landau, H. C., & Wang, M. M. (2021). Carbon cycling in mature and regrowth forests globally. *Environmental Research Letters*, 16(5), 053009. <https://doi.org/10.1088/1748-9326/abed01>

- Badorek, T., Tuittila, E. S., Ojanen, P., & Minkkinen, K. (2011). Forest floor photosynthesis and respiration in a drained peatland forest in southern Finland. *Plant Ecology and Diversity*, 4(2–3), 227–241. <https://doi.org/10.1080/17550874.2011.644344>
- Baldocchi, D. D. (2003). Assessing the eddy covariance technique for evaluating carbon dioxide exchange rates of ecosystems: Past, present and future. *Global Change Biology*, 9(4), 479–492. <https://doi.org/10.1046/j.1365-2486.2003.00629.x>
- Barr, A. G., Richardson, A. D., Hollinger, D. Y., Papale, D., Arain, M. A., Black, T. A., Bohrer, G., Dragoni, D., Fischer, M. L., Gu, L., Law, B. E., Margolis, H. A., Mccaughey, J. H., Munger, J. W., Oechel, W., & Schaeffer, K. (2013). Use of change-point detection for friction-velocity threshold evaluation in eddy-covariance studies. *Agricultural and Forest Meteorology*, 171, 31–45. <https://doi.org/10.1016/j.agrformet.2012.11.023>
- Buffam, I., Laudon, H., Temnerud, J., Mörth, C. M., & Bishop, K. (2007). Landscape-scale variability of acidity and dissolved organic carbon during spring flood in a boreal stream network. *Journal of Geophysical Research: Biogeosciences*, 112(G1), 218. <https://doi.org/10.1029/2006JG000218>
- Callesen, I., Raulund-Rasmussen, K., Westman, C. J., & Tau-Strand, L. (2007). Nitrogen pools and C:N ratios in well-drained Nordic forest soils related to climate and soil texture. *Boreal Environment Research*, 12, 681–692.
- Cannell, M. G. R., & Smith, R. I. (1986). Climatic warming, spring budburst and forest damage on trees. *Journal of Applied Ecology*, 23, 177–191.
- Chapin, F. S., Woodwell, G. M., Randerson, J. T., Rastetter, E. B., Lovett, G. M., Baldocchi, D. D., Clark, D. A., Harmon, M. E., Schimel, D. S., Valentini, R., Wirth, C., Aber, J. D., Cole, J. J., Goulden, M. L., Harden, J. W., Heimann, M., Howarth, R. W., Matson, P. A., McGuire, A. D., ... Schulze, E. D. (2006). Reconciling carbon-cycle concepts, terminology, and methods. *Ecosystems*, 9(7), 1041–1050. <https://doi.org/10.1007/s10021-005-0105-7>
- Clymo, R. S. (1984). The limits to peat bog growth. *Philosophical Transactions of the Royal Society of London. B, Biological Sciences*, 303(1117), 605–654.
- Cole, J. J., Prairie, Y. T., Caraco, N. F., McDowell, W. H., Tranvik, L. J., Striegl, R. G., Duarte, C. M., Kortelainen, P., Downing, J. A., Middelburg, J. J., & Melack, J. (2007). Plumbing the global carbon cycle: Integrating inland waters into the terrestrial carbon budget. *Ecosystems*, 10(1), 172–185. <https://doi.org/10.1007/s10021-006-9013-8>
- Eliasson, P. (2008). Skogsdikning och skogsväxt under 1900-talet. In L. Runefelt (Ed.), *Svensk mosskultur: Odling, torvanvändning och landskapets förändring 1750–2000* (pp. 181–195). Kungliga skogs- och lantbruksakademie.
- Evans, C. D., Renou-Wilson, F., & Strack, M. (2016). The role of waterborne carbon in the greenhouse gas balance of drained and rewetted peatlands. *Aquatic Sciences*, 78(3), 573–590. <https://doi.org/10.1007/s00027-015-0447-y>
- Finstad, A. G., Andersen, T., Larsen, S., Tominaga, K., Blumentrath, S., De Wit, H. A., Tømmervik, H., & Hessen, D. O. (2016). From greening to browning: Catchment vegetation development and reduced S-deposition promote organic carbon load on decadal time scales in Nordic lakes. *Scientific Reports*, 6(1), 1–8. <https://doi.org/10.1038/srep31944>
- Foken, T., Göockede, M., Mauder, M., Mahrt, L., Amiro, B., & Munger, W. (2004). Post-field data quality control. In X. Lee, W. J. Massman, & B. Law (Eds.), *Handbook of micrometeorology* (pp. 181–208). Springer. [https://doi.org/10.1007/1-4020-2265-4\\_9](https://doi.org/10.1007/1-4020-2265-4_9)
- Fratini, G., Sabbatini, S., Ediger, K., Riensche, B., Burba, G., Nicolini, G., Vitale, D., & Papale, D. (2018). Eddy covariance flux errors due to random and systematic timing errors during data acquisition. *Biogeosciences*, 15(17), 5473–5487. <https://doi.org/10.5194/bg-15-5473-2018>
- Frolking, S., Talbot, J., Jones, M. C., Treat, C. C., Kauffman, J. B., Tuittila, E. S., & Roulet, N. (2011). Peatlands in the Earth's 21st century climate system. *Environmental Reviews*, 19, 371–396. <https://doi.org/10.1139/a11-014>
- Gash, J. H. C., & Culf, A. D. (1996). Applying a linear detrend to eddy correlation data in realtime. *Boundary-Layer Meteorology*, 79(3), 301–306. <https://doi.org/10.1007/BF00119443>
- Hänell, B. (1991). *Forest classification of peatlands in Sweden - A field guide*. Swedish University of Agricultural Sciences.
- He, H., Jansson, P. E., Svensson, M., Björklund, J., Tarvainen, L., Klemetsson, L., & Kasimir, Å. (2016). Forests on drained agricultural peatland are potentially large sources of greenhouse gases – Insights from a full rotation period simulation. *Biogeosciences*, 13(8), 2305–2318. <https://doi.org/10.5194/bg-13-2305-2016>
- Hedwall, P. O., Skoglund, J., & Linder, S. (2015). Interactions with successional stage and nutrient status determines the life-form-specific effects of increased soil temperature on boreal forest floor vegetation. *Ecology and Evolution*, 5(4), 948–960. <https://doi.org/10.1002/ece3.1412>
- Hiraishi, T., Krug, T., Tanabe, K., Srivastava, N., Baasansuren, J., Fukuda, M., & Troxler, T. G. (2014). *2013 Supplement to the 2006 IPCC guidelines for national greenhouse gas inventories: Wetlands*. IPCC.
- IPCC. (2022). *Climate change 2022: Impacts, adaptation, and vulnerability*. Contribution of Working Group II to the Sixth Assessment Report of the Intergovernmental Panel on Climate Change (H.-O. Pörtner, D. C. Roberts, M. Tignor, E. S. Poloczanska, K. Mintenbeck, A. Alegria, M. Craig, S. Langsdorf, S. Löschke, V. Möller, A. Okem, & B. Rama, Eds.). Cambridge University Press. <https://doi.org/10.1017/9781009325844>
- Irvin, J., Zhou, S., McNicol, G., Lu, F., Liu, V., Fluet-Chouinard, E., Zutao, O., Helen, K. S., Antje, L.-M., Carlo, T., Dario, P., Domenico, V., Ivan, M., Pavel, A., Mika, A., Anand, A., Dennis, B., Sheel, B., Gil, B., ... Jackson, R. B. (2021). Gap-filling eddy covariance methane fluxes: Comparison of machine learning model predictions and uncertainties at FLUXNET-CH4 wetlands. *Agricultural and Forest Meteorology*, 308, 108528. <https://doi.org/10.1016/j.agrformet.2021.108528>
- Jocher, G., Marshall, J., Nilsson, M. B., Linder, S., De Simon, G., Hörnlund, T., Lundmark, T., Näsholm, T., Löfvenius, M. O., Tarvainen, L., Wallin, G., & Peichl, M. (2018). Impact of canopy decoupling and subcanopy advection on the annual carbon balance of a boreal scots pine forest as derived from eddy covariance. *Journal of Geophysical Research: Biogeosciences*, 123(2), 303–325. <https://doi.org/10.1002/2017JG003988>
- Joosten, H., & Clarke, D. (2002). *Wise use of mires and peatlands*. International Mire Conservation Group and International Peat Society.
- Kämäräinen, M., Lintunen, A., Kulmala, M., Tuovinen, J. P., Mammarella, I., Aalto, J., Vekuri, H., & Lohila, A. (2022). Evaluation of gradient boosting and random forest methods to model subdaily variability of the atmosphere–forest CO<sub>2</sub> exchange. *Biogeosciences Discussions*, 2022, 1–24. <https://doi.org/10.5194/bg-2022-108>
- Kasimir, Å., He, H., Coria, J., & Nordén, A. (2018). Land use of drained peatlands: Greenhouse gas fluxes, plant production, and economics. *Global Change Biology*, 24(8), 3302–3316. <https://doi.org/10.1111/gcb.13931>
- Kasimir, Å., He, H., Jansson, P. E., Lohila, A., & Minkkinen, K. (2021). Mosses are important for soil carbon sequestration in forested peatlands. *Frontiers in Environmental Science*, 383, 680430. <https://doi.org/10.3389/fenvs.2021.680430>
- Kljun, N., Calanca, P., Rotach, M. W., & Schmid, H. P. (2015). A simple two-dimensional parameterisation for Flux Footprint Prediction (FFP). *Geoscientific Model Development*, 8(11), 3695–3713. <https://doi.org/10.5194/gmd-8-3695-2015>
- Koehler, A. K., Sottocornola, M., & Kiely, G. (2011). How strong is the current carbon sequestration of an Atlantic blanket bog? *Global*

- Change Biology*, 17(1), 309–319. <https://doi.org/10.1111/j.1365-2486.2010.02180.x>
- Korkiakoski, M., Ojanen, P., Tuovinen, J. P., Minkkinen, K., Nevalainen, O., Penttilä, T., Aurela, M., Laurila, T., & Lohila, A. (2023). Partial cutting of a boreal nutrient-rich peatland forest causes radically less short-term on-site CO<sub>2</sub> emissions than clear-cutting. *Agricultural and Forest Meteorology*, 332, 109361.
- Korkiakoski, M., Tuovinen, J. P., Aurela, M., Koskinen, M., Minkkinen, K., Ojanen, P., Penttilä, T., Rainne, J., Laurila, T., & Lohila, A. (2017). Methane exchange at the peatland forest floor—automatic chamber system exposes the dynamics of small fluxes. *Biogeosciences*, 14(7), 1947–1967. <https://doi.org/10.5194/bg-14-1947-2017>
- Kulmala, L., Pumpanen, J., Kolari, P., Dengel, S., Berninger, F., Köster, K., Matkala, L., Vanhatalo, A., Vesala, T., & Bäck, J. (2019). Inter- and intra-annual dynamics of photosynthesis differ between forest floor vegetation and tree canopy in a subarctic Scots pine stand. *Agricultural and Forest Meteorology*, 271, 1–11. <https://doi.org/10.1016/j.agrformet.2019.02.029>
- Lafleur, P. M., Moore, T. R., Roulet, N. T., & Frolking, S. (2005). Ecosystem respiration in a cool temperate bog depends on peat temperature but not water table. *Ecosystems*, 8, 619–629. <https://doi.org/10.1007/s10021-003-0131-2>
- Laine, A. M., Mehtätalo, L., Tolvanen, A., Frolking, S., & Tuittila, E. S. (2019). Impacts of drainage, restoration and warming on boreal wetland greenhouse gas fluxes. *Science of the Total Environment*, 647, 169–181. <https://doi.org/10.1016/j.scitotenv.2018.07.390>
- Laine, J., Silvola, J., Tolonen, K., Alm, J., Nykänen, H., Vasander, H., Sallantausta, T., Savolainen, I., Sinisalo, J., & Martikainen, P. J. (1996). Effect of water-level drawdown on global climatic warming: Northern peatlands. *Ambio*, 25, 179–184.
- Laine, J., Vasander, H., & Laiho, R. (1995). Long-term effects of water level drawdown on the vegetation of drained pine mires in southern Finland. *Journal of Applied Ecology*, 32, 785–802.
- Laudon, H., Berggren, M., Ågren, A., Buffam, I., Bishop, K., Grabs, T., Jansson, M., & Köhler, S. (2011). Patterns and dynamics of dissolved organic carbon (DOC) in boreal streams: The role of processes, connectivity, and scaling. *Ecosystems*, 14, 880–893. <https://doi.org/10.1007/s10021-011-9452-8>
- Laudon, H., & Hasselquist, E. M. (2023). Applying continuous-cover forestry on drained boreal peatlands; water regulation, biodiversity, climate benefits and remaining uncertainties. *Trees, Forests and People*, 11, 100363. <https://doi.org/10.1016/j.tfp.2022.100363>
- Leach, J. A., Larsson, A., Wallin, M. B., Nilsson, M. B., & Laudon, H. (2016). Twelve year interannual and seasonal variability of stream carbon export from a boreal peatland catchment. *Journal of Geophysical Research: Biogeosciences*, 121(7), 1851–1866. <https://doi.org/10.1002/2016JG003357>
- Leskinen, P., Cardellini, G., González-García, S., Hurmekoski, E., Sathre, R., Seppälä, J., Smyth, C., Stern, T., & Verkerk, P. J. (2018). Substitution effects of wood-based products in climate change mitigation. *From Science to Policy*. <https://doi.org/10.36333/fs07>
- Lindroth, A., Holst, J., Linderson, M. L., Aurela, M., Biermann, T., Heliasz, M., Chi, J., Ibrom, A., Kolari, P., Klemetsson, L., Krasnova, A., Laurila, T., Lehner, I., Lohila, A., Mammarella, I., Mölder, M., Löfvenius, M. O., Peichl, M., Pilegaard, K., ... Nilsson, M. (2020). Effects of drought and meteorological forcing on carbon and water fluxes in Nordic forests during the dry summer of 2018. *Philosophical Transactions of the Royal Society B*, 375(1810), 20190516. <https://doi.org/10.1098/rstb.2019.0516>
- Livingston, G. P., & Hutchinson, G. L. (1995). Enclosure-based measurement of trace gas exchange: Applications and sources of error. In P. A. Matson & R. C. Harriss (Eds.), *Biogenic trace gases: Measuring emissions from soil and water* (pp. 14–51). Blackwell Science Inc.
- Lohila, A., Laurila, T., Aro, L., Aurela, M., Tuovinen, J. P., Laine, J., Kolari, P., & Minkkinen, K. (2007). Carbon dioxide exchange above a 30-year-old Scots pine plantation established on organic-soil crop-land. *Boreal Environment Research*, 12, 141–157.
- Lohila, A., Minkkinen, K., Aurela, M., Tuovinen, J. P., Penttilä, T., Ojanen, P., & Laurila, T. (2011). Greenhouse gas flux measurements in a forestry-drained peatland indicate a large carbon sink. *Biogeosciences*, 8(11), 3203–3218. <https://doi.org/10.5194/bg-8-3203-2011>
- Mao, R., Zhang, X., Song, C., Wang, X., & Finnegan, P. M. (2018). Plant functional group controls litter decomposition rate and its temperature sensitivity: An incubation experiment on litters from a boreal peatland in northeast China. *Science of the Total Environment*, 626, 678–683. <https://doi.org/10.1016/j.scitotenv.2018.01.162>
- Meyer, A., Tarvainen, L., Noursratpour, A., Björk, R. G., Ernfors, M., Grelle, A., Klemetsson, Å. K., Lindroth, A., Rantfors, M., Rütting, T., Wallin, G., Weslien, P., & Klemetsson, L. (2013). A fertile peatland forest does not constitute a major greenhouse gas sink. *Biogeosciences*, 10(11), 7739–7758. <https://doi.org/10.5194/bg-10-7739-2013>
- Minkkinen, K., Ojanen, P., Penttilä, T., Aurela, M., Laurila, T., Tuovinen, J. P., & Lohila, A. (2018). Persistent carbon sink at a boreal drained bog forest. *Biogeosciences*, 15(11), 3603–3624. <https://doi.org/10.5194/bg-15-3603-2018>
- Minkkinen, K., Penttilä, T., & Laine, J. (2007). Tree stand volume as a scalar for methane fluxes in forestry-drained peatlands in Finland. *Boreal Environment Research*, 12, 127–132.
- Moore, T. R. (2003). Dissolved organic carbon in a northern boreal landscape. *Global Biogeochemical Cycles*, 17(4), 2050. <https://doi.org/10.1029/2003GB002050>
- Moosavi, S. C., & Crill, P. M. (1997). Controls on CH<sub>4</sub> and CO<sub>2</sub> emissions along two moisture gradients in the Canadian boreal zone. *Journal of Geophysical Research: Atmospheres*, 102(D24), 29261–29277. <https://doi.org/10.1029/96JD03873>
- Neubauer, S. C., & Megonigal, J. P. (2021). Biogeochemistry of wetland carbon preservation and flux. In K. W. Krauss, Z. Zhu, & C. L. Stagg (Eds.), *Wetland carbon and environmental management* (pp. 33–71). American Geophysical Union. <https://doi.org/10.1002/9781119639305.ch3>
- Nieminen, M., Sarkkola, S., Sallantausta, T., Hasselquist, E. M., & Laudon, H. (2021). Peatland drainage—a missing link behind increasing TOC concentrations in waters from high latitude forest catchments? *Science of the Total Environment*, 774, 145150. <https://doi.org/10.1016/j.scitotenv.2021.145150>
- Nilsson, M., Sagerfors, J., Buffam, I., Laudon, H., Eriksson, T., Grelle, A., Klemetsson, L., & Lindroth, A. (2008). Contemporary carbon accumulation in a boreal oligotrophic minerogenic mire – A significant sink after accounting for all C-fluxes. *Global Change Biology*, 14(10), 2317–2332. <https://doi.org/10.1111/j.1365-2486.2008.01654.x>
- Noumonvi, K. D., Ågren, A. M., Ratcliffe, J. L., Öquist, M. G., Ericson, L., Tong, C. H. M., Järveoja, J., Zhu, W., Osterwalder, S., Peng, H., Erefur, C., Bishop, K., Laudon, H., Nilsson, M. B., & Peichl, M. (2023). The Kulbäcksliden research infrastructure: A unique setting for northern peatland studies. *Frontiers in Earth Science*, 11, 1194749. <https://doi.org/10.3389/feart.2023.1194749>
- Ojanen, P., & Minkkinen, K. (2020). Rewetting offers rapid climate benefits for tropical and agricultural peatlands but not for forestry-drained peatlands. *Global Biogeochemical Cycles*, 34(7), e2019GB006503. <https://doi.org/10.1029/2019GB006503>
- Ojanen, P., Minkkinen, K., Alm, J., & Penttilä, T. (2010). Soil–atmosphere CO<sub>2</sub>, CH<sub>4</sub> and N<sub>2</sub>O fluxes in boreal forestry-drained peatlands. *Forest Ecology and Management*, 260(3), 411–421. <https://doi.org/10.1016/j.foreco.2010.04.036>
- Ojanen, P., Minkkinen, K., & Penttilä, T. (2013). The current greenhouse gas impact of forestry-drained boreal peatlands. *Forest Ecology and Management*, 289, 201–208. <https://doi.org/10.1016/j.foreco.2012.10.008>

- Olsson, M. (1999). *Soil survey in Sweden*. Soil Resources of Europe. Joint Research Centre.
- Paavilainen, E., & Päävänä, J. (1995). *Peatland forestry: Ecology and principles* (Vol. 111). Springer Science & Business Media.
- Palviainen, M., Peltomaa, E., Laurén, A., Kinnunen, N., Ojala, A., Berninger, F., Zhu, X., & Pumpanen, J. (2022). Water quality and the biodegradability of dissolved organic carbon in drained boreal peatland under different forest harvesting intensities. *Science of the Total Environment*, 806, 150919. <https://doi.org/10.1016/j.scitotenv.2021.150919>
- Pastor, J., Solin, J., Bridgham, S. D., Updegraff, K., Harth, C., Weishampel, P., & Dewey, B. (2003). Global warming and the export of dissolved organic carbon from boreal peatlands. *Oikos*, 100(2), 380–386. <https://doi.org/10.1034/j.1600-0706.2003.11774.x>
- Peacock, M., Audet, J., Bastviken, D., Futter, M. N., Gauci, V., Grinham, A., Harrison, J. A., Kent, M. S., Kosten, S., Lovelock, C. E., Veraart, A. J., & Evans, C. D. (2021). Global importance of methane emissions from drainage ditches and canals. *Environmental Research Letters*, 16(4), 044010. <https://doi.org/10.1088/1748-9326/abeb36>
- Peichl, M., Öquist, M., Löfvenius, M. O., Ilstedt, U., Sagerfors, J., Grelle, A., Lindroth, A., & Nilsson, M. B. (2014). A 12-year record reveals pre-growing season temperature and water table level threshold effects on the net carbon dioxide exchange in a boreal fen. *Environmental Research Letters*, 9(5), 055006. <https://doi.org/10.1088/1748-9326/9/5/055006>
- Ranniku, R., Schindler, T., Escuer-Gatius, J., Mander, Ü., Machacova, K., & Soosaar, K. (2023). Tree stems are a net source of CH<sub>4</sub> and N<sub>2</sub>O in a hemiboreal drained peatland forest during the winter period. *Environmental Research Communications*, 5(5), 051010. <https://doi.org/10.1088/2515-7620/acd7c7>
- Ratcliffe, J. L., Campbell, D. I., Clarkson, B. R., Wall, A. M., & Schipper, L. A. (2019). Water table fluctuations control CO<sub>2</sub> exchange in wet and dry bogs through different mechanisms. *Science of the Total Environment*, 655, 1037–1046. <https://doi.org/10.1016/j.scitotenv.2018.11.151>
- Ratcliffe, J. L., Creevy, A., Andersen, R., Zarov, E., Gaffney, P. P., Taggart, M. A., Mazei, Y., Tsyganov, A. N., Rowson, J. G., Lapshina, E. D., & Payne, R. J. (2017). Ecological and environmental transition across the forested-to-open bog ecotone in a west Siberian peatland. *Science of the Total Environment*, 607, 816–828.
- Rebmann, C., Kolle, O., Heinesch, B., Queck, R., Ibrom, A., & Aubinet, M. (2012). Data acquisition and flux calculations. In M. Aubinet, T. Vesala, & D. Papale (Eds.), *Eddy covariance* (pp. 59–83). Springer. <https://doi.org/10.1016/j.scitotenv.2017.06.276>
- Reichstein, M., Falge, E., Baldocchi, D., Papale, D., Aubinet, M., Berbigier, P., Buchmann, C. B. N., Gilmanov, T., Granier, A., Grünwald, T., Havránková, K., Ilvesniemi, H., Janous, D., Knohl, A., Laurila, T., Lohila, A., Loustau, D., Matteucci, G., Meyers, T., ... Valentini, R. (2005). On the separation of net ecosystem exchange into assimilation and ecosystem respiration: Review and improved algorithm. *Global Change Biology*, 11(9), 1424–1439. <https://doi.org/10.1111/j.1365-2486.2005.001002.x>
- Richardson, A. D., & Hollinger, D. Y. (2007). A method to estimate the additional uncertainty in gap-filled NEE resulting from long gaps in the CO<sub>2</sub> flux record. *Agricultural and Forest Meteorology*, 147(3–4), 199–208. <https://doi.org/10.1016/j.agrformet.2007.06.004>
- Roulet, N. T., Lafleur, P. M., Richard, P. J., Moore, T. R., Humphreys, E. R., & Bubier, J. I. L. L. (2007). Contemporary carbon balance and late Holocene carbon accumulation in a northern peatland. *Global Change Biology*, 13(2), 397–411. <https://doi.org/10.1111/j.1365-2486.2006.01292.x>
- Sallinen, A., Akanegbu, J., Marttila, H., & Tahvanainen, T. (2023). Recent and future hydrological trends of aapa mires across the boreal climate gradient. *Journal of Hydrology*, 617, 129022. <https://doi.org/10.1016/j.jhydrol.2022.129022>
- Sikström, U., & Hökkä, H. (2016). Interactions between soil water conditions and forest stands in boreal forests with implications for ditch network maintenance. *Silva Fennica*, 50, 1416. <https://doi.org/10.14214/sf.1416>
- Silvola, J. (1986). Carbon dioxide dynamics in mires reclaimed for forestry in eastern Finland. *Annales Botanici Fennici*, 23, 59–67.
- Sjörs, H. (1990). Divergent successions in mires, a comparative study. *Aquilo, Serie Botanica*, 28, 67–77.
- Skogsstyrelsen. (2021). *Klimatpåverkan från dikad torvtäckt skogsmark – effekter av dikesunderhåll och återvätning*. Report No. 2021/7.
- Thomas, C. K., Martin, J. G., Law, B. E., & Davis, K. (2013). Toward biologically meaningful net carbon exchange estimates for tall, dense canopies: Multi-level eddy covariance observations and canopy coupling regimes in a mature Douglas-fir forest in Oregon. *Agricultural and Forest Meteorology*, 173, 14–27. <https://doi.org/10.1016/j.agrformet.2013.01.001>
- Tong, C. H. M., Nilsson, M. B., Sikström, U., Ring, E., Drott, A., Eklöf, K., Futter, M. N., Peacock, M., Segersten, J., & Peichl, M. (2022). Initial effects of post-harvest ditch cleaning on greenhouse gas fluxes in a hemiboreal peatland forest. *Geoderma*, 426, 116055. <https://doi.org/10.1016/j.geoderma.2022.116055>
- Treat, C. C., Bubier, J. L., Varner, R. K., & Crill, P. M. (2007). Timescale dependence of environmental and plant-mediated controls on CH<sub>4</sub> flux in a temperate fen. *Journal of Geophysical Research: Biogeosciences*, 112(G1), 210. <https://doi.org/10.1029/2006JG000210>
- Turetsky, M., Wieder, K., Halsey, L., & Vitt, D. (2002). Current disturbance and the diminishing peatland carbon sink. *Geophysical Research Letters*, 29(11), 14000. <https://doi.org/10.1029/2001GL014000>
- Vainio, E., Haikarainen, I. P., Machacova, K., Putkinen, A., Santalahti, M., Koskinen, M., Fritze, H., Tuomivirta, T., & Pihlatie, M. (2022). Soil-tree-atmosphere CH<sub>4</sub> flux dynamics of boreal birch and spruce trees during spring leaf-out. *Plant and Soil*, 478(1–2), 391–407. <https://doi.org/10.1007/s11104-022-05447-9>
- Vekuri, H., Tuovinen, J. P., Kulmala, L., Papale, D., Kolari, P., Aurela, M., Laurila, T., Liski, J., & Lohila, A. (2023). A widely-used eddy covariance gap-filling method creates systematic bias in carbon balance estimates. *Scientific Reports*, 13(1), 1720. <https://doi.org/10.1038/s41598-023-28827-2>
- Wallin, M., Buffam, I., Öquist, M., Laudon, H., & Bishop, K. (2010). Temporal and spatial variability of dissolved inorganic carbon in a boreal stream network: Concentrations and downstream fluxes. *Journal of Geophysical Research: Biogeosciences*, 115(G2), 1100. <https://doi.org/10.1029/2009JG001100>
- Wallin, M. B., Grabs, T., Buffam, I., Laudon, H., Ågren, A., Öquist, M. G., & Bishop, K. (2013). Evasion of CO<sub>2</sub> from streams – The dominant component of the carbon export through the aquatic conduit in a boreal landscape. *Global Change Biology*, 19(3), 785–797. <https://doi.org/10.1111/gcb.12083>
- Wallin, M. B., Öquist, M. G., Buffam, I., Billett, M. F., Nisell, J., & Bishop, K. H. (2011). Spatiotemporal variability of the gas transfer coefficient (KCO<sub>2</sub>) in boreal streams: Implications for large scale estimates of CO<sub>2</sub> evasion. *Global Biogeochemical Cycles*, 25(3), 3975. <https://doi.org/10.1029/2010GB003975>
- Webb, J. R., Santos, I. R., Maher, D. T., & Finlay, K. (2019). The importance of aquatic carbon fluxes in net ecosystem carbon budgets: A catchment-scale review. *Ecosystems*, 22(3), 508–527. <https://doi.org/10.1007/s10021-018-0284-7>
- Welp, L. R., Randerson, J. T., & Liu, H. P. (2007). The sensitivity of carbon fluxes to spring warming and summer drought depends on plant functional type in boreal forest ecosystems. *Agricultural and Forest Meteorology*, 147(3–4), 172–185. <https://doi.org/10.1016/j.agrformet.2007.07.010>
- Wilczak, J. M., Oncley, S. P., & Stage, S. A. (2001). Sonic anemometer tilt correction algorithms. *Boundary-Layer Meteorology*, 99(1), 127–150. <https://doi.org/10.1023/A:1018966204465>



- Wutzler, T., Lucas-Moffat, A., Migliavacca, M., Knauer, J., Sickel, K., Šigut, L., Menzer, O., & Reichstein, M. (2018). Basic and extensible post-processing of eddy covariance flux data with REddyProc. *Biogeosciences*, 15(16), 5015–5030. <https://doi.org/10.5194/bg-15-5015-2018>
- Yrjälä, K. I. M., Tuomivirta, T., Juottonen, H., Putkinen, A., Lappi, K., Tuittila, E. S., Penttilä, T., Minkkinen, K., Laine, J., Peltoniemi, K., & Fritze, H. (2011). CH<sub>4</sub> production and oxidation processes in a boreal fen ecosystem after long-term water table drawdown. *Global Change Biology*, 17(3), 1311–1320. <https://doi.org/10.1111/j.1365-2486.2010.02290.x>

## SUPPORTING INFORMATION

Additional supporting information can be found online in the Supporting Information section at the end of this article.

**How to cite this article:** Tong, C. H. M., Noumonvi, K. D., Ratcliffe, J., Laudon, H., Järveoja, J., Drott, A., Nilsson, M. B., & Peichl, M. (2024). A drained nutrient-poor peatland forest in boreal Sweden constitutes a net carbon sink after integrating terrestrial and aquatic fluxes. *Global Change Biology*, 30, e17246. <https://doi.org/10.1111/gcb.17246>